The Pennsylvania State University

The Graduate School

Department of Civil and Environmental Engineering

IDENTIFYING BALLAST FOULING USING STATISTICAL PATTERN RECOGNITION TECHNIQUES ON SMARTROCK DATA

A Thesis in

Civil Engineering

by

Saharnaz Nazari

Submitted in Partial Fulfillment

of the Requirements

for the Degree of

Master of Science

May 2018

The thesis of Saharnaz Nazari was reviewed and approved* by the following:

Patrick Fox

John A. and Harriette K. Shaw Professor

Head of the Department of Civil Engineering

Hai Huang

Associate Professor of Rail Transportation Engineering

Thesis Co-Advisor

Tong Qiu

Associate Professor of Civil Engineering

Thesis Co-Advisor

Shihui Shen

Associate Professor of Rail Transportation Engineering

Xinli Wu

Assistant Professor of Engineering Design

*Signatures are on file in the Graduate School

Abstract

Railroad ballast serves different functions including draining water from track and distribution of the train loads. The ballast layer deteriorates and becomes fouled with time due to ballast particle abrasion and breakage as well as subgrade soil intrusion. Ballast fouling has become one of the most commonly seen track defects that can lead to inconsistent track performance. In the case of fouling, the ballast strength will decrease when it is wet (usually referred to as "mud-spot") due to the lack of particle interlocking and lubrication effect of fine materials. However, both of the ballast strength and stiffness will increase dramatically when it is in dry condition as the ballast particles are well confined (Qian, 2016). This inconsistency in track behavior can cause higher deterioration rate of other track components such as rail and sleeper. Therefore, identifying mud spots in a timely manner is a critical issue in ballasted track maintenance.

The main purpose of this thesis is using advanced sensor networks and statistical pattern recognition techniques to identify ballast fouling by studying the relationship between ballast fouling condition and ballast particle movement. To that end, several field experiments were carried out with the aim of monitoring and recording the particle movements under different ballast conditions. In particular, two sections with the same traffic but different track conditions: one with clean ballast and the other with mud pumping, were chosen. The SmartRock (Liu, 2015) is used to obtain ballast particle movement information under traffic. The SmartRock is a wireless sensor device built using the 3D printing technology and resembles the real ballast particles in terms of shape, inter particle friction and specific gravity. This sensor device has the ability to record translational and rotational movement of a single ballast particle under dynamic loading and transfer the real-time data via Bluetooth to a base station. The autoregressive (AR) model was then applied to each of the acceleration and rotation time histories collected from the SmartRocks embedded in the two sections, during which the autoregressive coefficients will be obtained. Those coefficients will serve as damage indicators to identify ballast fouling severities. The results and important findings are highlighted in this thesis.

Keywords: Ballast Fouling, Railway, SmartRock, Statistical Pattern Recognition Analysis

Table of Contents

List of Figures

List of Tables

Acknowledgments

First and foremost, I shall express my highest level of gratitude to my thesis advisors, Dr. Huang and Dr. Qiu, for their constant help and encouragement. Dr. Huang has provided me the opportunity to work on this thesis subject matter by providing me the great insights on the subject as well as the necessary data to conduct the statistical analysis. This research would not have been possible without him. Dr. Qiu has been truly supportive since the first day.

Additionally, my sincere thanks go to the thesis committee members, Dr. Shen and Dr. Wu for their time and assistance.

I would also like to thank my dear friends in the Civil Department, Shushu and Kun for their support while I was doing my thesis. I shall also thank my dear friend Yassi for her help.

Finally, this thesis owes largely to the support of my family who are so close despite being physically so far away. I would like to dedicate my heartfelt thank you to them for their constant support and for their many sacrifices that allowed me to be where I am today.

1 Introduction

1.1 Background

Rail transportation is considered as one of the most economic and efficient modes of transportation for both passengers and freight. A typical railroad track (Figure 1-1) has two structural components: superstructure including rail, fasteners and sleeper and substructure consisting of ballast, sub-ballast, and subgrade.

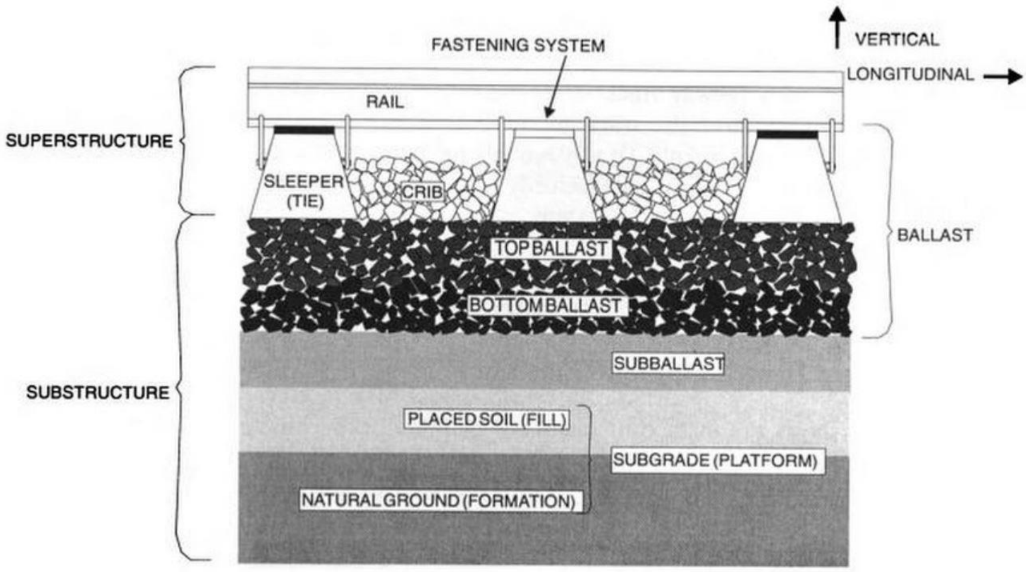

Figure 1-01: Track structure components (Selig and waters, 1994)

The Ballast layer, depending on their locations within a track, can be divided into 3 main parts. The part between two adjacent ties which is called crib; the part outside the end of ties which are called shoulder ballast; and the part under the bottom of the tie (Zarembski, 2014).

The function of ballast layer includes but not limited to: distributing the train vertical load to protect the subgrade and providing drainage. In this regard, the ballast layer plays a key role in track performance. Various criteria including ballast layer thickness, particle size, and distribution can affect the ability of the ballast to fulfill its own function (Li, 2015).

Fouling is the condition when the voids in ballast become occupied by the smaller particles generated mainly from the ballast particle breakage. It is believed to significantly affect the stiffness and strength of the ballast. (Indraratna et al., 2013) Therefore, frequent evaluation of ballast and monitoring its condition are necessary from the efficiency and safety point of view.

Particle size distribution, normally obtained by sieve analysis, is one of the most common approaches to evaluate the ballast condition. A gap graded ballast assembly will create large enough voids to provide the track with proper drainage. A typical ballast grain size distribution suggested by AREMA is depicted in the following figure.

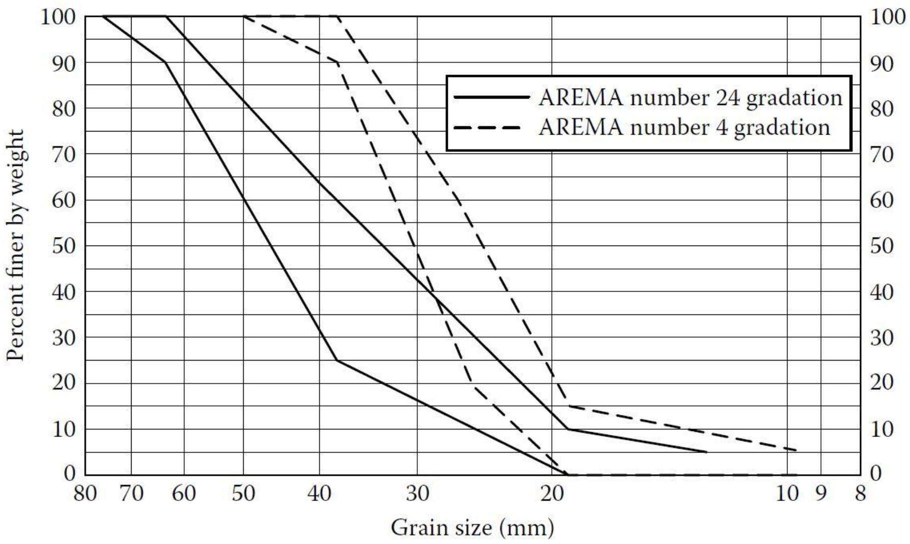

Figure1- 2: #24 and #4 ballast particle gradation ranges based on AREMA (LI, 2015)

Although sieve analysis offers ground truth for the severity of ballast fouling, it is time consuming to conduct onsite sampling and sieving, not even mention the interruption of the daily traffic operation. A non-destructive and real time monitoring system with advanced statistical algorithms to accurately detect ballast fouling in a timely manner is in great need.

Nowadays, the inspection and monitoring of the structures are of a great interest in the railway area. A great number of advanced sensors and technologies have been developed in order to achieve more efficient inspection and monitoring system. These emerging technologies provide a vast amount of data from real-time monitoring of track infrastructure. Extracting efficient knowledge required for the maintenance planning from these data is the next challenge.

1.2 Research Objective

The primary objective of this research is to develop an algorithm for evaluating the ballast condition through real-time particle movement data recorded using the SmartRock. This objective is reached by applying the statistical pattern recognition techniques on the data collected from two different structural conditions of ballasted track in order to find the best damage detection approach.

1.3 Outline

This thesis is presented in five chapters. Chapter 1 includes an introduction to the subject and research objectives. Chapter 2 presents a literature review of the current state of research in ballast fouling and structural health monitoring. Chapter 3 describes the procedures for site selection and the instrumentation plan of the project. Chapter 4 presents the analysis procedure in order to develop the damage detection algorithm and the result of applying these analyses on the data collected from the field. Chapter 5 provides suggestions for future research.

2 Literature Review

2.1 Previous studies on ballast fouling

ballast layer consists of "the uniformly graded angular material" and is the top layer in the track substructure. This layer's main function is distribution of train loads and also draining water from the superstructure. The ballast gradation is a key factor in achieving the drainage task. According to Selig and Waters, a few of these factors affecting the ballast gradation are the following:

1) "Mechanical particle degradation during construction and maintenance work, and under traffic loading"

2) "Chemical and mechanical weathering degradation from environmental changes"

3) "Migration of fine particles from the surface and the underlying layers" (Selig and Waters, 1994)

Fouling is an unfavorable condition for the ballast layer in a railroad track, detrimentally affecting the ballast performance. Fouling can be described as the condition in which the voids between the ballast particles in a ballast layer become occupied by smaller materials or fouling agents, commonly resulting from "ballast particle breakage or from subgrade soil intrusion, or from the contamination coming from outside of the track such as coal dust" (Huang, 2011). The finer fouling particles fill the void spaces between the ballast particles; as the percentage of these tiny fouling particles increases, the fouling can lead to the loss of the ballast layer's open-graded characteristics and therefore the loss of drainage capacity. Internal studies conducted by railroad companies have found that "Breaking the ballast aggregate commonly generates almost all fouling fines in the railroad track" (CN 1987).

According to Selig and Waters, the share of each source of fouling in a ballasted track is as follows: "on the average, up to 76% of the ballast fouling is due to ballast particle breakage; the second factor is infiltration from subballast that accounts for 13% of fouling; 7% infiltration from ballast surface; 3% subgrade intrusion; and 1% due to tie wear." (Selig and Waters, 1994)

In terms of the stability and load bearing capacity of ballast layer, Huang and his colleagues (Huang et al., 2009) mentioned three various stages of ballast layer fouling based on the volume of fine materials in the void space of ballast. Figure 2-3(a) shows a ballast sample that is clean or very slightly fouled (Phase I), in which the load is carried by the ballast particle surface interaction. As shown in Figure 2-3(b), ballast fouling will reach Phase II when the number of fine particles increases to the point where the voids in between aggregates are filled; however, all the aggregates are still in contact with each other. At the ultimate level of fouling (Phase III), the particles lose their surface contact as a result of the increased number of fine particles. In this condition, the finer particles are those that define the particle movements (see Figure 2-3(c)). In order to better plan for maintenance activities like ballast cleaning, it is worth studying the point when ballast enters the second phase of fouling and how each fouling agent and fine particle volume will affect the ballast layer's physical properties. (Huang et al., 2009).

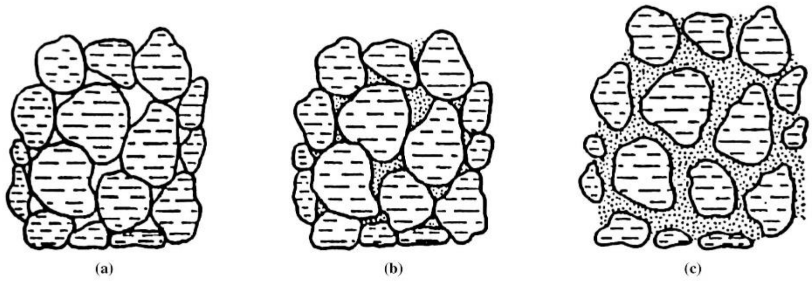

Figure 2-3: ballast fouling phases: (a) Phase I (clean ballast), (b) Phase II (partially fouled ballast), and (c) Phase III (heavily fouled ballast) (Huang et al., 2009)

Several studies have attempted to quantify the level of fouling and have introduced methods for assessing the ballast fouling condition. Fouling index (FI), as suggested by Selig and Waters (Selig, 1994), is a parameter that defines ballast fouling based on ballast particles' gradations. It can be calculated by the following equation:

$$FI = P_4 + P_{200} \tag{1}$$

In this equation, P_4 and P_{200} are defined as the percentages of ballast particles passing the sieve size number 4 (4.75 mm) and number 200 (0.075 mm), respectively. An index related to FI is the percentage of fouling (% fouling), which is the ratio of the dry weight of material passing a 9.5 mm sieve to the dry weight of the total sample (Selig and Waters,1994). A limitation of this method is that the type of fouling material is not considered in developing the parameter. Therefore, evaluating a fouling situation based on FI is not applicable for all materials. In cases that ballast fouled by a great percentage of particles finer than 0.075 mm, for instance, care should be taken (Indraratna, 2011).

Feldman and Nissen (2002) considered the void reduction in ballast due to fouling and presented the Percentage Void Contamination (PVC) parameter:

$$PVC = \frac{V_{vf}}{V_{vb}} * 100 \tag{2}$$

where V_{vb} is defined as the total volume of void exist between ballast particles and V_{vf} is the total volume of fouling material (particles passing 9.5 mm sieve), in the re-compacted ballast (Feldman, 2002). The problems with this approach is that the volume measurement is time-consuming. Moreover, the author did not take the distribution of fouling particles into account, which could result in an overestimation of the fouling level (Indraratna, 2011).

Indraratna et al. (2011) studied the existing approaches for estimating the fouling level in ballast, such as FI and PVC, and as a result of this study, another parameter is developed. This parameter called the relative ballast fouling ratio, (R_{bf}) which can be defined by the following equation:

$$R_{bf} = \frac{M_f * \left({}^{G_{b-f}}\!/\!_{G_{s-f}} \right)}{M_b} * 100\% \tag{3}$$

This parameter is the ratio of the fouling particles volume to the volume of ballast particles. The sieve size 9.5 mm separates fouling material and ballast particles. In this equation, *M* is the dry mass and *G*s is specific gravity. Subscripts *f* and *b* define whether the variable refers to ballast properties or to the fouling material. Following this study, the authors also defined levels of fouling based on the three most common fouling parameters including relative ballast fouling ratio, FI and PVC. The results are demonstrated in Table 2-1 (Indraratna, 2011).

Table 2-1: levels of fouling based on the common fouling parameters (Indraratna, 2011)

Category	Fouling index (Selig and Waters 1994) (%)	Percentage of fouling (%)	Relative ballast fouling ratio (%)
Clean	<1	<2	<2
Moderately clean	1 to <10	2 to <9.5	2 to <10
Moderately fouled	10 to <20	9.5 to <17.5	10 to <20
Fouled	20 to <30	17.5 to <34	20 to <50
Highly fouled	≥40	≥34	≥50

A study by Tennakoon et al. (Tennakoon et al., 2012) examined the change in ballast draining capacity due to fouling. This study introduced a modification to the PVC called the void contamination index (VCI). This new parameter defines the percentage of the total ballast voids occupied by the fouling material and considers the effect of various aspects of both the fouling material and bllast layer including gradations, void ratios, and specific gravities:

$$VCI = \frac{1+e_f}{e_b} * \frac{G_{sb}}{G_{sf}} * \frac{M_f}{M_b} * 100 \qquad (4)$$

where

e_b is void ratio of clean ballast; e_f is fouling material void ratio; G_{sb} is specific gravity of clean ballast; G_{sf} is specific gravity of fouling material; M_b is dry mass of clean ballast; and M_f is dry mass of fouling material (Tennakoon et al., 2012).

the authors attempted to relate the hydraulic conductivity of fouled to the VCI parameter. To do so, a series of “large-scale constant-head hydraulic conductivity tests” were carried out on ballast samples with changing the stages of fouling. As a result of this study, a design chart was established (figure 2-4) to offer guidelines for decision-making regarding ballast maintenance. The experimental studies concluded that an increase in VCI results in the decrease of hydraulic conductivity. The chart illustrates that track maintenance measures should begin when the clay fouled ballast reaches a VCI over 50%, which is considered critical condition. The authors found that a small increase in VCI will decrease the ballast hydraulic conductivity significantly until VCI reaches a limit of 50% and 90% for the fouling materials coal and clay, respectively. Beyond this point, the hydraulic conductivity of fouled ballast can be considered equal to that of the fouling material itself (Tennakoon, 2012).

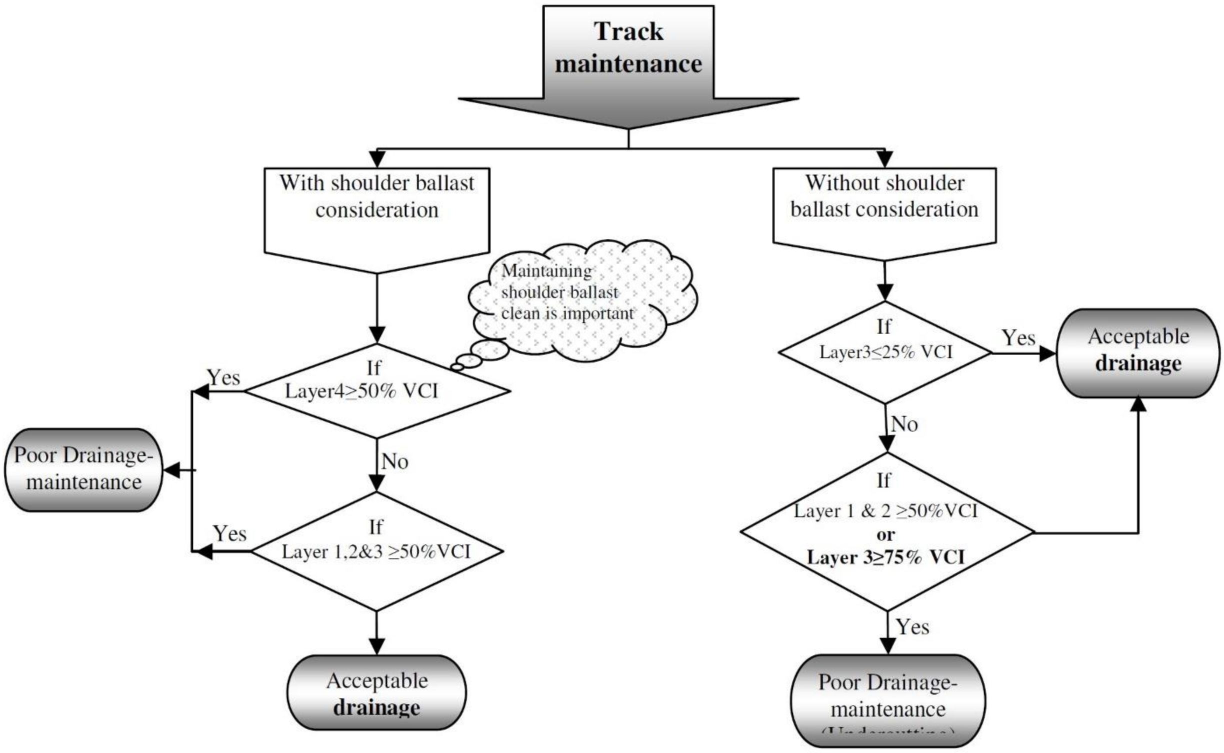

Figure 2-4: flow chart for ballast maintenance decision making (Tennakoon, 2012)

A 2009 study by Huang et al. investigated the strength and also deformation features of ballast material made up of granite (Huang et al., 2009). The authors applied large direct shear (shear box) tests on two groups of samples, one with clean ballast and the other with samples of ballast fouled by different materials. The fouling agents in this study included "Coal dust, plastic clay, and non-plastic mineral filler" (Huang et al., 2009). Based on the results of the direct shear tests, this study concluded that fouling could affect the shear strength by decreasing the friction angles and cohesion intercepts of samples and that, as a result, the shear strengths were lower compared with the clean ballast samples. Samples tested under wet conditions had lower ballast shear strengths in comparison to the sample fouled with dry Coal dust. The most severe reductions in shear strength were in the coal dust sample at high fouling levels. An appropriate point to begin maintenance measures was determined to be 15% dry coal dust fouling by weight of ballast, a level sufficient to cause critical fouling and make a considerable reduction in the ballast strength (Huang et al. ,2009).

Huang et al. in 2011 conducted another study investigating the field performance of track fouled by coal dust. In this study, the authors chose coal dust as the fouling material in consideration of past study results, stating, Coal dust fouling agent has the most detrimental effect on ballast strength. For analysis of the results, a numerical method called “image-aided discrete element modeling (DEM)” was used (Huang et al. ,2009). Based on the authors’ explanation, “the DEM is a modeling appropriate for solving problems that express discontinuous behavior and the general behavior of a granular assembly will be defined by modeling the particles individually and stimulating their motion. This behavior which may include permanent deformations, dilation, and anisotropy, is modeled implicitly.” In this study, a ballasted track was simulated using DEM approach to investigate the track settlement for two various fouling scenarios, fouling in track shoulder and also in track center, under repeated loading. Prior to the DEM simulation, Direct shear strength tests were done on the clean and coal dust fouled samples in order to validate the DEM simulation model results and define the various parameters in the model to make it consistent with the results of the corresponding laboratory tests. (Huang et al., 2011)

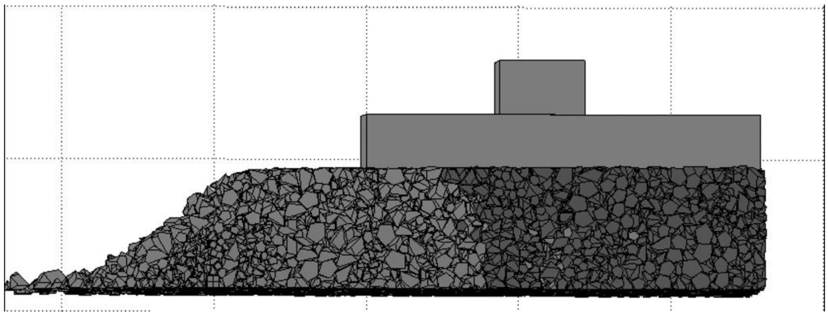

Figure2- 5: coal dust fouled Half-track DEM model (Huang et al., 2011)

The results of this study demonstrated that shoulder fouling had the worst effect on track settlement regardless of the level of fouling (partially or fully fouled ballast). Moreover, it was observed that fouled samples had higher settlement potential than clean ballast samples. In other words, the authors concluded, "within a relatively short amount of time, a fouled part of the track will accumulate more settlement comparing to the clean part. This issue may lead to the scenario often referred as "hanging tie"" (illustrated in Figure 2-6) (Huang et al., 2011).

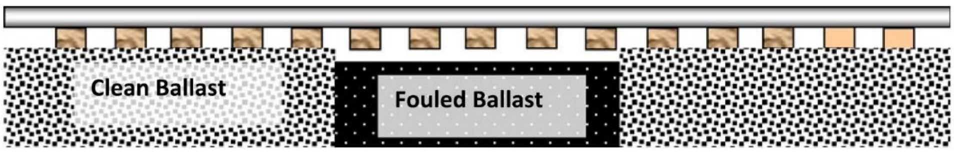

Figure 2-6: Hanging tie happened as a result of ballast fouling (Huang et al., 2011)

This section has reviewed the various studies previously conducted to examine the effect of fouling on ballast behavior. All previous ballast fouling studies focused on particle size and material properties. However, as a direct cause of track instability, ballast particle movement (or movability) has never been studied. For this reason, the development of a continuous monitoring system that would give insight into ballast particle movement in real time would improve the maintenance and efficiency of the track operation. The current study uses remote sensors called SmartRock (explained in detail later in this chapter) in an attempt to record the ballast particle movement in a section of track with fouled ballast and in another section with clean ballast. Ultimately, an algorithm for detecting fouling in ballast through interpretation of the SmartRock data is proposed.

2.2 Previous studies on structural health monitoring (SHM)

Structural Health Monitoring (SHM) is a research topic that currently has wide application in mechanical, aerospace, and civil engineering. Many structures continue to operate despite their aging, and damage will potentially accumulate in these structures. Therefore, monitoring and tracking their structural condition is increasingly important and crucial for safety and economic reasons. Therefore, improving efficiency and developing an effective maintenance plan are incentives for research in the area of SHM. The main purpose of SHM is to distinguish, locate, and evaluate structural damage through the changes in structural response (Samwanshi, 2016).

From a civil engineering standpoint, SHM is an efficient and effective approach for providing an infrastructure asset management system in order to support and maintain social interactions and economic development. structural deterioration with age seems inevitable, and failure of such civil infrastructure can have important harmful impacts on society. Therefore, the current situation of these structures must be understood and managed in order to preserve their functional integrity and serviceability(Samwanshi, 2016).

Visual inspection is one of the common methods of detecting structural anomalies but is expensive and time-consuming. An SHM method employing a wireless sensor network (WSN) not only enhances the safety and reliability of civil infrastructure but also decreases the amount of time and money spent on structural monitoring, helping to facilitate maintenance planning and decision making (Samwanshi, 2016).

In a 1999 study, Farrar et al. discussed "vibration-based damage detection" as one of the approaches that has been a main focus of research related to structural monitoring.

Sohn (2001) asserts:

> "Damage identification based upon variation in dynamic response is one of the few methods that monitor changes in the structure on a global basis. The foundation of vibration-based damage diagnosis is that any alteration in the physical properties will cause changes in the measured dynamic response of the structure" (Sohn, 2001).

Farrar pointed out that in the process of employing a strategy for making a distinction between damaged and undamaged structures, the term "damage" should be defined (Farrar, 1999). Generally, damage can be explained by comparing the two different conditions of the structure. In this regard, changes in the response measurements compared to the initial and often undamaged state can be interpret as damage in the system (Farrar, 1999).

In an article published in 1999, Farrar et al. stated that the SHM problems can be fundamentally explained through statistical pattern recognition.

In their review of SHM studies, Sohn et al. state:

> "The damage identification in the statistical pattern recognition framework can be described as a four-step process:
>
> (1) Operational Evaluation,
>
> (2) Data Acquisition, Fusion, and Cleansing,
>
> (3) Feature Extraction and Information Condensation
>
> (4) Statistical Model Development for Feature Discrimination" (Sohn, 2002)

Based on the above definitions of damage and the pattern recognition approach, the process of structural health monitoring includes recognizing what damage can potentially occur in the structure, then observing the system over a period of time and measuring the response periodically. In the next step, the damage-sensitive features should be extracted from the measurements; the condition of the structure can then be determined by analyzing those features. The functionality of the system despite degradation caused by the aging and operational environments should be measured periodically in order to obtain updated information as the output of SHM (Farrar, 1999). Figure 2-7 demonstrates the steps of SHM in the framework of pattern recognition. Each step is then summarized in the discussion that follows (Farrar, 1999).

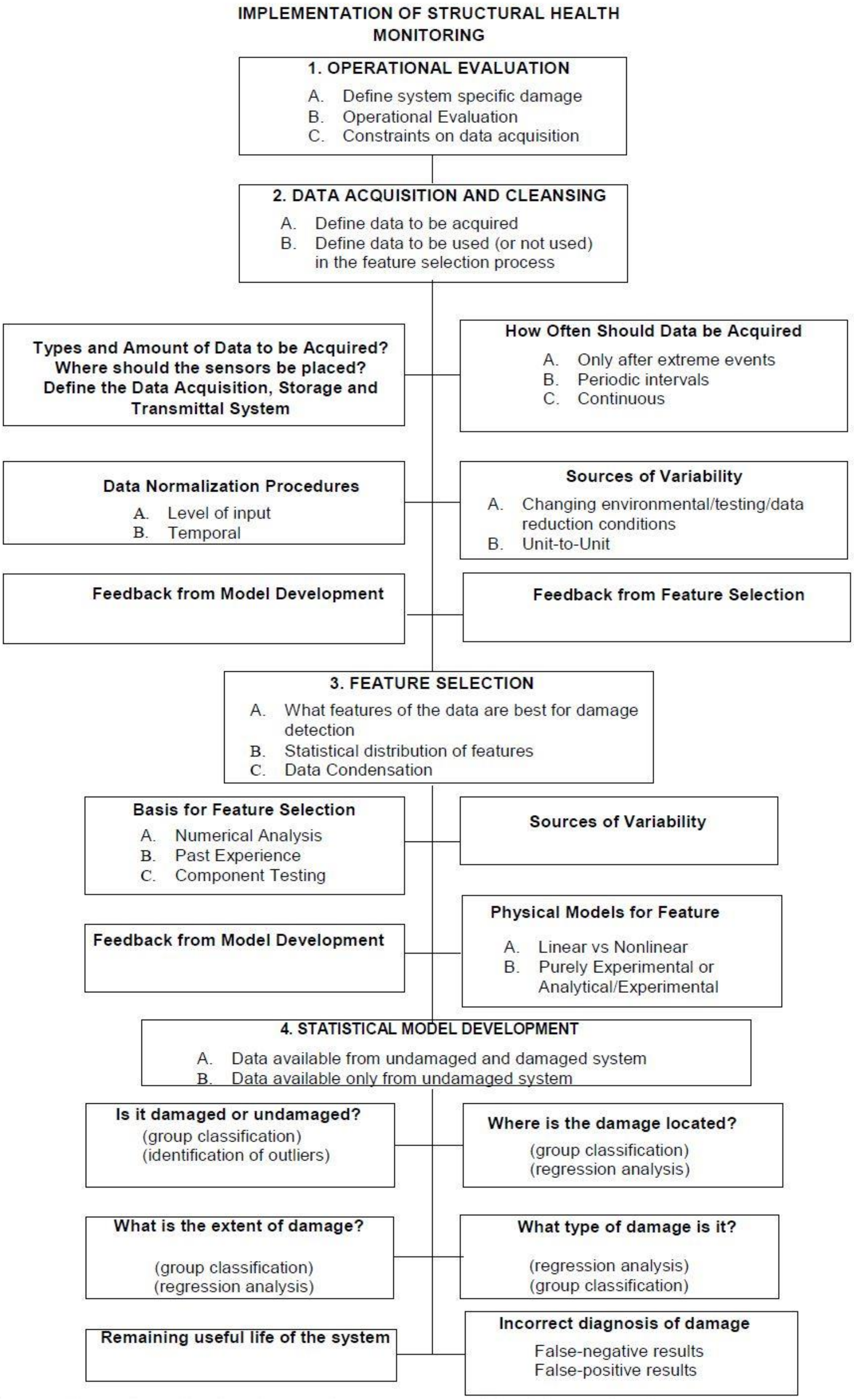

Figure 2-7: Flow chart for the sequence of applying a SHM program (Farrar, 1999)

Operational evaluation

first step mentioned by Sohn et al. in SHM is operational evaluation. This step consider the safety or economic benefit of the monitoring in the structure of interest and the limitations exist for data collection. Most of the previous studies on SHM neglected to discuss this step because they took place in a laboratory environment with no considerable operational or environmental inconsistency. In these studies, the damage was created through a controlled approach and the safety or economic motivations for monitoring the system were not a focus of the researchers' attention.

The authors believed that this step should be emphasized in order for SHM to move from being a theoretical research topic to being applicable in the real world (Sohn et al., 2002).

Data acquisition and cleansing

Sohn et al. (2002) explain this part of the structural health monitoring procedure as follows:

> "This aim of this step is to define the types of sensors, their placement, the number of sensors to be used, and also the data acquisition system and data collection frequency."

The conditions of environment and the way the structure is used can cause significant variations in the dynamic features of the structure, the environmental and operational effects "can disguise the changes caused by structural deterioration" (Gul, 2009). In mitigation, by "normalizing any obtained data prior to selecting the damage sensitive feature, the signal changes caused by operational and environmental alteration of the system can be distinguished from structural deterioration or degradation" (Sohn, 2001).

Feature extraction and information condensation

This step includes defining and deriving the appropriate damage-sensitive features that enable us to make distinctions between the data coming from undamaged and damaged structural responses.

A huge amount of data is produced as a result of various technologies used to monitor and measure the system response and damage diagnosis. The difference between the data related to various stages of the structure's health condition is not always straightforward to detect. Therefore, features that are sensitive to the changes in data and happened as a result of damage should be defined. The features for anomaly detection typically depend on the system application, and numerous features are often recognized for a structure and gathered into a "feature vector" (Sohn et al., 2002). Data compression is an inherent part of feature extraction. As a result of this step, data compresses into the small-dimension feature vectors that simplify the evaluation of their distribution and anomaly detection. Generally, a low dimensional feature vector is preferable (Sohn et al., 2002).

Statistical model development

The statistical model development focuses on developing the algorithms to define the damage condition of the system using the features extracted prior to this step. As a result of the SHM, based on the level of knowledge that must be acquired from the structure, the purpose of damage detection can be defined as locating the damage, severity, and type of damage and in the system and, ultimately, determining the remaining useful life of the structure (Farrar, 1999).

A 2002 paper by Sohn et al. (Sohn et al., 2002) reviewed the previous studies conducted on SHM. The authors categorize the algorithm for analyzing the monitoring into three approaches that vary based on whether the data from both the undamaged and damaged conditions of the structure are obtainable at the time of analysis. The class of algorithms appropriate for instances where data from both conditions of the system is available is supervised learning, including group classification and regression analysis. Unsupervised learning algorithms should be applied when the data does not contain information from the damaged condition. Finally, a significant part of the statistical process is examining models developed based on real data in order to determine the model's sensitivity and prediction accuracy for the selected damage indicator feature. In this step, the likelihood of false indications of damage is studied.

According to Sohn (Sohn, 2001), there are two types of false damage warning:

1) "False-positive damage indication (the indication of damage when none is present)"

2) "False-negative damage indications (no indication of damage when damage is present)"

Brownjohn et al. conducted a study in 2007 concerning the problems and limitations in the advancement of civil infrastructure monitoring systems.

They asserted:

> "Some key problems exist on the way to safe and effective automation of structural monitoring and maintenance managing through SHM approaches. This issues that need to be considered include but are not limited to maintaining the low-cost for the maintenance and monitoring system, defining the critical locations in the structure for

damage detection, determining the best plan for sensor placement and efficient sensor distribution and considering the environmental factors and noises that disturb the effective damage diagnosis process.” (Brownjohn, 2007)

2.2.1 The statistical analysis approaches for defect detection

From life-safety and financial viewpoints, the capability of monitoring the structural health of many mechanical, civil, and aerospace engineering structures has become increasingly important, since these systems continue to be used in spite of their age and the related risk of damage occurring (Sohn, 2001).

After selecting the appropriate feature for damage indication in the structural health monitoring procedure, regression, classification, and outlier detection are the most common statistical models used to distinguish the difference between the feature of a control data and the damaged one. The algorithms in this step can be classified into two main groups, supervised and unsupervised. The supervised algorithm requires data from both damaged and undamaged structures, while the unsupervised algorithm requires only undamaged structure data. It can be concluded from the discussion above that the unsupervised algorithms are preferred, since data from both the damaged and undamaged condition is not available for all structures in the real world. The statistical model should make a distinction between the features developed in the last step to recognize the damage occurrence (Sohn, 2002).

2.2.1.1 Statistical pattern recognition

In the domain of SHM and damage identification, one of the most popular methodologies among scholars is statistical pattern recognition. The majority of the SHM studies employing statistical pattern recognition apply an amalgamation of “the time series analysis with a statistical detection methods (outlier detection)” (Gul, 2009).

Gul (2009) examined the statistical pattern recognition methods for detecting the structural change on “a highly redundant steel grid structure.” In the experiment, the test specimen was densely instrumented with 12 accelerators. The ambient vibration was created by “random hand tapping”. While applying various damage situations to the test structure, the acceleration data was collected. In this study, the author used autoregressive (AR) model coefficients as damage indicator features. Prior to applying the AR model, Gul processed the data by using normalized random decrement (RD) in order to “eliminate the effect of random loading obtaining free decay response.” In the next step, the 10th order of the AR model was fitted based on the result of the partial autocorrelation function (PACF). The feature vectors that formed the steps of this approach are illustrated schematically in Figure 2-8.

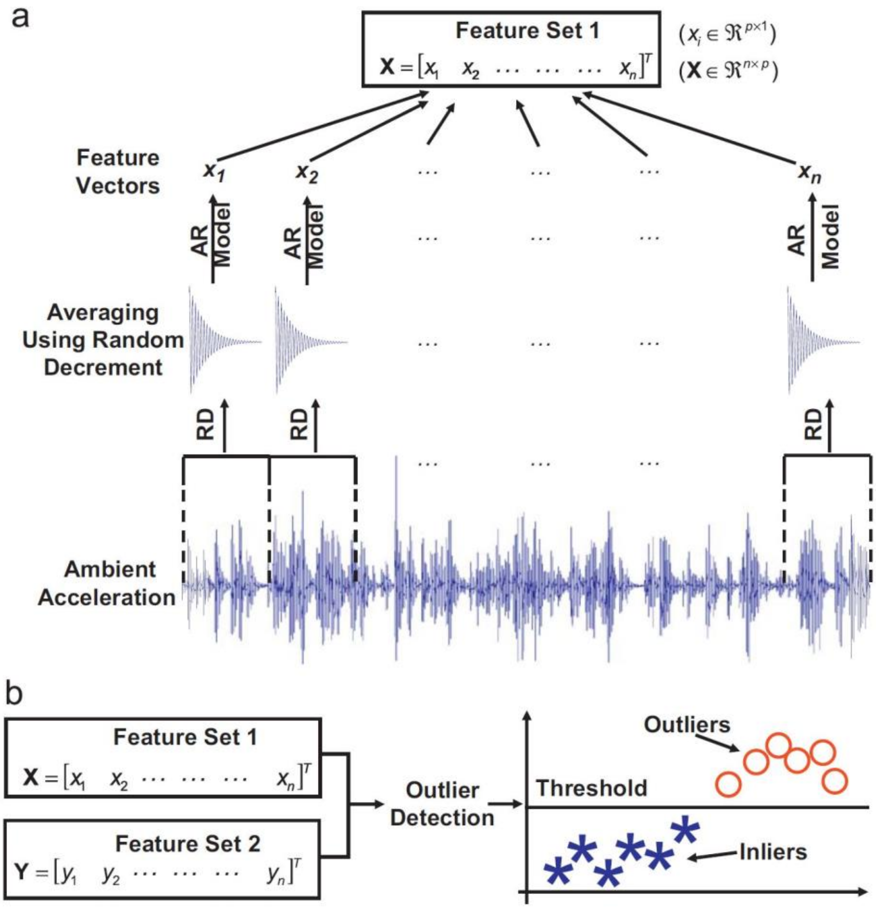

Figure 2-8: Summary of the methodology: (a) forming feature vector using AR model and (b) outlier detection of the obtained features (Gul, 2009)

The subsequent step was the outlier detection, for which the Mahalanobis distance method was used to set thresholds to identify the changes in the structure. The results indicated that this methodology is generally capable of detecting damage, because when the severity of the damage increases, the number of false negatives decreases. Figure 2-9 illustrates an example of the results of this study related to the Scour case—the most severe type of damage. It is notable that the scour is clearly recognized as a changed structural state, subsequently all the features related to the damaged condition are above the threshold rate (Gul, 2009).

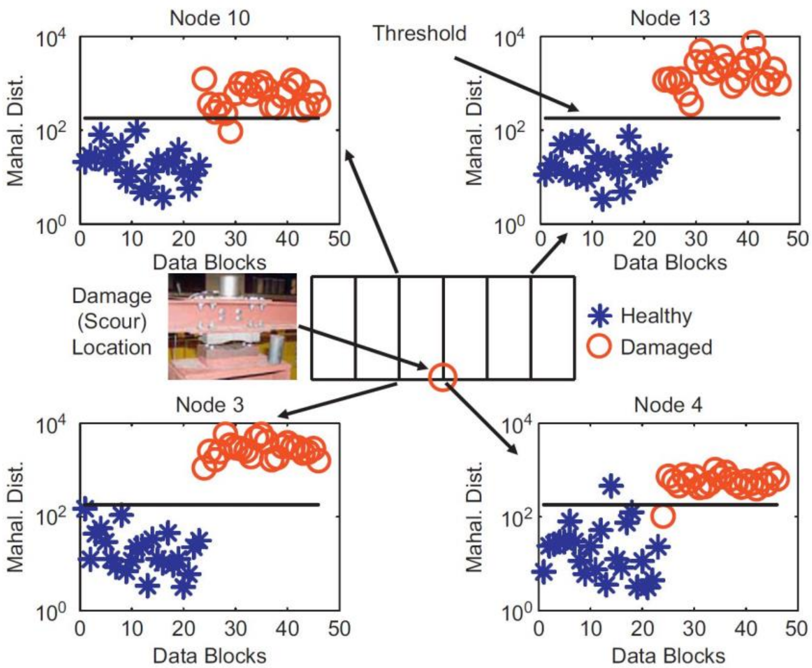

Figure 2-9:outlier detection using Mahalanobis distance (Gul, 2009)

In another study by Sohn et al. (2000), the authors attempted to apply statistical pattern recognition techniques to distinguish the plastic deformation in a bridge's concrete column. For this, a concrete column was built in the lab. A load was applied to that column in five different levels of damage, and data was collected by forty accelerometers attached to the column. The time history data collected from the experiment went through the pattern recognition steps in order to build up an algorithm capable of determining the damage in the column. Since the experiment was done in the lab environment, there was no source of variation in data in terms of operational and environmental conditions. First, a third-order autoregressive (AR) model was fit to the recorded time histories as the damage-indicator feature. The autoregressive model is a regression in time series data that predicts a value of time series data based on the previous values. The general p order form of AR is shown by the equation as below:

$$x(t) = \sum_{j=1}^{p} \varphi_{xj} x(t-j) + e_x(t) \quad (6)$$

In this equation, e is the random error, and ϕ is the AR coefficient (Sohn, 2000).

With the aim of damage indication, a technique called statistical process control (SPC) referred to as an ''X-bar control chart'' was applied to the feature vector. A control chart offers a statistical framework for observing forthcoming quantities and measurements to assure the new data is consistent with the past data. Control limits of the X-bar control chart were based on the attributes acquired from the original structure. Lastly, the AR coefficients of the models that were fit to the subsequent new data were monitored comparative to the control limits. A sign indicating a system shifting from a healthy state to a damaged state is when a statistically significant number of features are outside the control limits (Sohn, 2000).

In this study (Sohn, 2000) plotting X-bar control chart using the single AR coefficient did not clearly indicate the damage in the structure. To enhance the model, various projection techniques like linear or quadratic projection and PCA were applied to the feature vectors. The discriminant analysis is a process that defines the combination of the features to project the multidimensional AR coefficients into a 1D feature space and maximize the class separation.

Sohn et al. (2000) explained in more detail their projection technique as the last stage of their study:

> "[…] prior to feature extraction, PCA is applied on all response data in order to reduce the data's dimension. That is, all the time series from multiple measurement points are projected onto the first principal component, and the subsequent feature selection is performed using this compressed time series. This technique improved the accuracy of control chart analysis compared to the damage detection with utilizing only the individual AR coefficient" (Sohn, 2000).

The final result of this experiment is illustrated in Figure 2-10. It is notable that in the higher level of damage, the outlier is significantly increased.

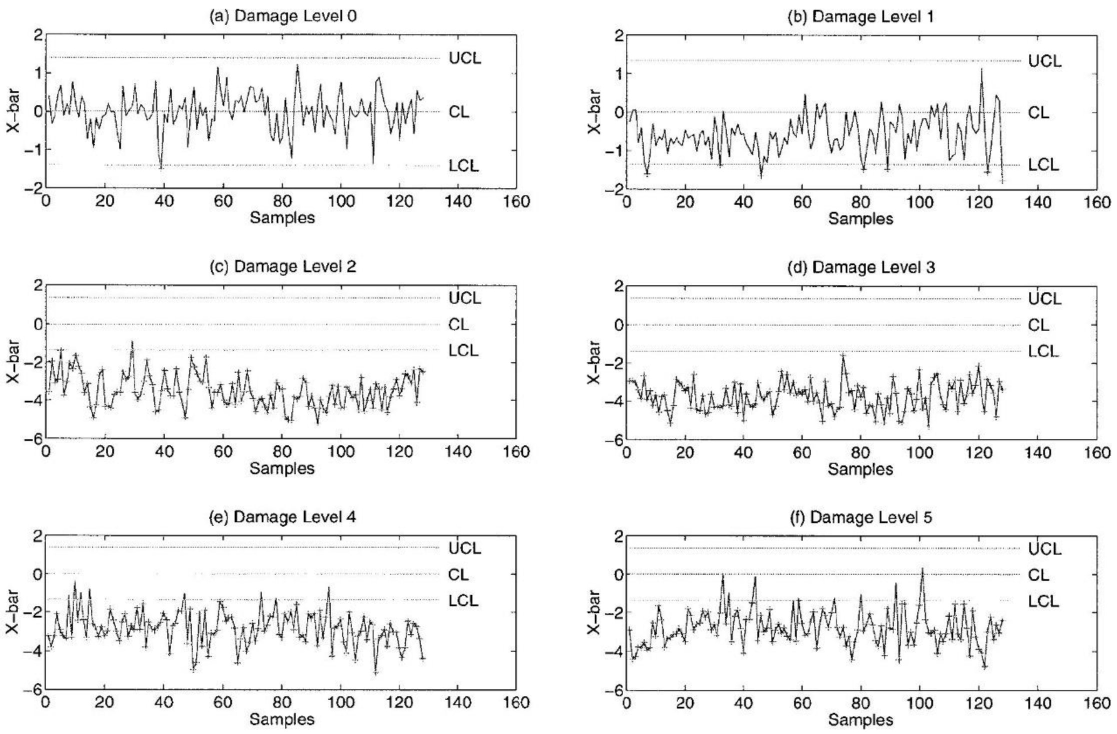

Figure 2-10: The outlier detection using the X-bar chart for the AR coefficient (Sohn, 2000)

Sohn et al. conducted a study (Sohn, 2001) on three strain signals collected from two various structural situations of a “surface-effect fast patrol boat” using “fiber optic strain gauges”. The first two sets of signals (Signals 1 and 2) were captured when the structural condition was the same, but Signal 3 was recorded in a dissimilar structural condition than Signals 1 and 2.

What makes this study unique compared to the other SHM studies is that data was collected under varying environmental and operational conditions including but not limited to sea states, the thermal condition related to water and air, and ship speed. In the first step of this study, “a novel data normalization approach, combining AR and AR with exogenous inputs (ARX) techniques, is developed so that the effect of structural damage could be separated from the effects of environmental and operational conditions (Sohn, 2001).”

More specifically, this procedure begins by assuming that there are previously recorded signals acquired from “unknown operational and environmental condition but from known structural condition,” and, based on the result of the autocorrelation function, a 30-order autoregressive (AR) model is applied to them. An AR model will also be developed for a newly obtained signal from unknown structural condition(Sohn, 2001).

As a result, if a new signal (assume y(t)) and the one recorded from a known structural condition ((x(t)) are from the same operational and environmental condition, the following difference will be minimized:

$$difference = \sum_{j=1}^{p}(\varphi_{xj} - \varphi_{yj})^2 \quad (7)$$

Two features are employed for the damage indication in this study (Sohn, 2001). First, an ARX model is applied in order to create the input/output connection between ex(t) and x(t) in the AR model. The standard deviation ratio of the residual errors ($^{\sigma(\mathcal{E}_y)}/_{\sigma(\mathcal{E}_x)}$) is considered the damage-sensitive feature (Sohn, 2001). The equation below explains this:

$$\mathcal{E}_x(t) = x(t) - \sum \alpha_i\big(x(t-i)\big) - \sum \beta_i e_x\,(t-j) \quad (8)$$

In above equation α is the AR coefficient, e is random error, and ε is the residual error for the AR model. This approach yields the results displayed in Figure 2-11 (Sohn, 2001).

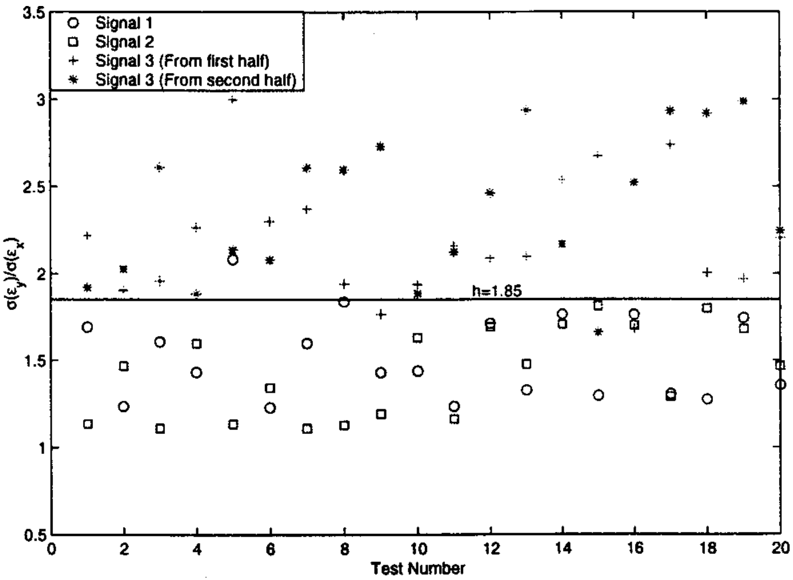

Figure 2-11: discrimination of the 3 signals using the ARX residual errors(Sohn, 2001)

Another statistical analysis that can be used on these 30-dimensional AR coefficient vectors is Mahalanobis distance. The Mahalanobis squared distance measure is given in the following equation used as the discordance test:

$$D_{\zeta} = \left(X_{\zeta} - \bar{X}\right)^{T} S^{-1} (X_{\zeta} - \bar{X}) \tag{9}$$

Where X_{ζ} is the possible outlier, $\bar{X}$ is the mean of the sample observation, and S is the covariance matrix. The result of this outlier detection is shown in Figure 2-12, which reveals that this approach proved to be efficient in distinguishing Signals 1 and 2 from the undamaged structure and Signal 3 from the damaged one (Sohn, 2001).

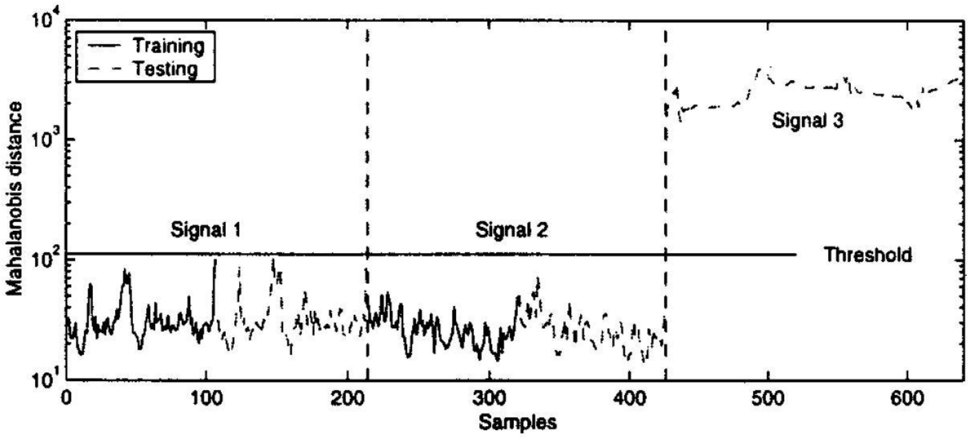

Figure 2-12: threshold for damage detection with the Mahalanobis criteria (Sohn, 2001)

In another study by Farrar et al. (1999), the test structure was a concrete bridge column subjected to quasi-static cyclic loading, with forty accelerometers mounted on it record data. The authors describe their methodology for defining damage-sensitive attribute as follows:

> "Third-order AR model coefficients was selected as the damage indicators. For the statistical analysis a group classification method called linear discriminant operator referred to as "fisher's discriminant" was introduced. As illustrated in Figure 2-13, when Fisher's discriminant is applied to data from the vibration tests conducted on the undamaged columns and from the vibration tests conducted after the first level of damage, there is a statistically significant separation between the LPC coefficients for the undamaged and damaged cases." (Farrar, 1999)

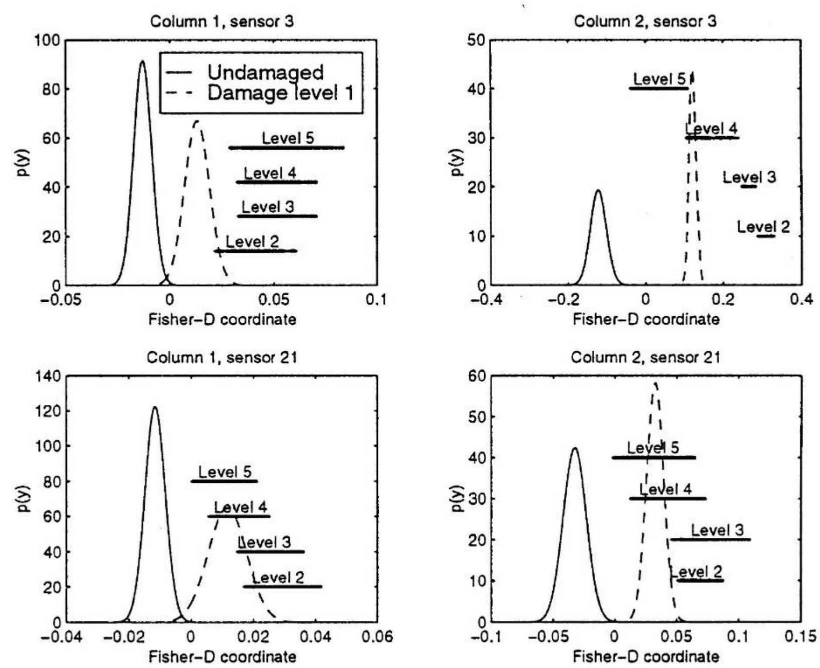

Figure 2-13: Distribution of feature produced using LPC mapped onto the Fisher coordinate (Farrar, 1999)

Data from both the undamaged and damaged structures is required to be available for applying this group classification method, while other statistical models that detect outliers can be used when data are available only from the undamaged structure. A significant aspect of classification is that a probability of damage is assigned, which can be used to rank systems for inspection in order of priority. (Farrar, 1999)

2.3 Ballast inspection

Railroad track inspection is a requirement for ensuring a safe track performance. A scheduled traditional visual track inspection is labor intensive, time-consuming, and sometimes is not able to detect defects in time. For these reasons, the international railroad community has begun noteworthy research with the aim of developing advanced technologies using cameras, sensors, computer processors, and other techniques to improve the inspection process, better plan for maintenance, and move towards the automatization of inspection tasks.

The ballast layer plays a vital role in track stability and in maintaining proper track geometry and should therefore be considered during track inspection. Conventional methods of ballast inspection have included regular visual assessment to look for signs of deficiency such as fouling or water accumulation and controlling the ballast gradation with lab sieve analysis. More recently, new inspection technologies that depend on the geometry of cars and on the gage, alignment, level, and modulus of the track have helped us understand deteriorated or failed ballast and/or subgrade conditions (Zarembski, 2014).

Today, new inspection technologies including ground-penetrating radar (GPR), LIDAR, and cone penetrometers enable inspectors to obtain more accurate insights into the ballast and substructure condition.

The name LIDAR is an abbreviation for Light Detection and Ranging or Laser Imaging Detection and Ranging. The technique employs optical remote sensing technology capable of measuring the distance to targets as well as other properties of objects. The mechanism of LIDAR involves the illumination of the target by laser light and the analysis of the backscattered light. In the railroad industry, LIDAR technology has been used "in measuring and mapping the surface of the track, and in particular, the ballast profile of the track structure" (Zarembski, 2014).

The technique of GPR can be used to identify the ballast condition as well as the condition of sub-ballast and subgrade. The goal of GPR is to locate "potentially problematic areas for further evaluation or maintenance." Due to the drastic changes in track conditions over a short distance, GPR can be considered "an optimal tool for the inspection of the ballast and subgrade. GPR can be used to identify trapped water areas with low bearing capacity, inappropriate ballast thickness, fouled ballast, and permanent deformations in the subgrade" (Zarembski, 2014).

A cone penetrometer is another technology for "a standard soil test procedure that has been adapted for use in inspection of ballast and subgrade conditions. Cone penetration test (CPT) is used to directly measure stiffness, strength, and thickness of the substructure layers" (Zarembski, 2014).

In recent years, various creative systems have been developed to monitor and inspect the condition of rail tracks and railway track components beyond the technologies discussed above. Researchers at the Institute of Intelligent Systems for Automation (ISSIA) in Italy are working on a system for detecting a defect within the ballast surface using 2D images captured by high-definition cameras and converting them to 3D images. The methods used for processing the images demand high computational power; therefore, these methods are expensive and not particularly feasible. Hence, the goal of future work will be "improving the analysis technique in order to make the system feasible for revenue service" (Camargo, 2011).

The past several years has witnessed a rapid "expansion in condition monitoring of systems, structures, vehicles, and machinery using sensors" due to the wide production of sensing technologies with low price. (Hodge, 2015) In a 2015 paper, Hodge reviewed the range of WSNs used for inspection and condition monitoring in the railway industry (Hodge, 2015). Until recently, inspection had been conducted visually. Visual inspection has several limitations, including the fact that objects could be examined only superficially and intermittently and that "the analysis needs to be interpreted by an expert, who can be subjective" (Hodge, 2015). In contrast to humans, "sensors are objective and can provide data from the entire object (including internally) to allow the whole object's health to be fully assessed and to analyze its durability and remaining lifetime" (Hodge, 2015). Table 2-2 demonstrates the broad range of railway monitoring sensors that provide an extensive range of data and allow monitoring of different structures, vehicles, and machinery.

Table2- 2: various common sensors in railway monitoring (Hodge,2015)

Object monitored	Measurement	Sensor
Bridge	Crack/Fatigue Detection	Acoustic Emission
	Stresses	Strain Gauge
		Piezoelectric Strain Gauge
		Fiber Bragg Strain Gauge
		Ultrasonic Strain
	Weight (of Train)	Strain Gauge
	Vibrations (Dynamic Load)	Accelerometer
Tunnel	Structure Distortion	Inclinometers
	Structure Movement	Displacement Transducers
	Vertical Displacement	Pressure Transducer
	Transverse Deformation	Pressure Transducer
Track	Crack/Fatigue Detection	Acoustic Emission
	Out of Round Wheel	Acoustic Emission
		Accelerometer
	Stresses	Strain Gauge
		Piezoelectric Strain Gauge
		Fiber Bragg Strain Gauge
	Vibrations (Dynamic Load)	Accelerometer
		Fiber Bragg
	Settlement and Twist	Inclinometer
	Incline	Inclinometer
Rail bed	Dynamic Acceleration (Track)	Accelerometers
	Pore Pressure (Ground Water)	Piezometers
	Pore Pressure (Ground Water)	Tensiometers
	Pore Pressure	Wire Potentiometers
	Long Term Settlement (Track)	Settlement Probes
	Temperature	Temperature Sensors (Thermistor)
	Vertical Motion	Extensometer
	Water Content	Reflectometer
	Movement / shape (of rail bed)	Accelerometers mounted in arm
Track infrastructure	Pressure	Piezoresistive Pressure Sensors
	Strain	Fiber Bragg Strain Gauge
	Displacement	Magnetic

2.3.1 SmartRock

Dr. Hai Huang, an associate professor at the Pennsylvania State University designed a wireless sensor called SmartRock which provides the possibility of studying the translational and rotational movement of ballast particles. (Liu, 2015)

The comparison of the shape of a SmartRock with a real ballast particle and also the DEM model built in order to develop the SmartRock and the internal unit of the SmartRock is depicted in figure 2-14.

Figure 2-14: SmartRock comparison to real ballast (Liu, 2015)

The SmartRock design was developed using the DEM element to resemble a real ballast particle in terms of shape, and then “3D-printing technology” was used in its production (Huang 2010). In order to enable the SmartRock to measure the rotation, translation, and orientation movement of a ballast particle with a maximum sampling frequency of 500 Hz, “a sensor with 9 degrees of freedom made up of a tri-axial gyroscope, a tri-axial accelerometer, and a tri-axial magnetometer was placed as the internal unit.” The raw data collected using the SmartRock can be sent to a base station wirelessly via Bluetooth, and the data can either be processed there or kept as time-stamped files within the SmartRock.

The features of the SmartRock wireless sensor are as follows:

<u>On-board sensors</u>

- Triple axis gyroscope – Selectable range up to 2000°/s.
- Triple axis accelerometer –Selectable range up to 8 g
- Triple axis magnetometer
- Thermometer
- Battery voltage level
- Calibrated real-time clock

- Selectable data rates up to 128 Hz

On-board algorithms

- 6-axis and 9-axis algorithms provide real-time measurement of orientation relative to the Earth

Connectivity

- USB
- Bluetooth – Class 1, 100m range
- Flash data storage

Power options

- USB – lightening charging
- LiPo battery – On-board charging
- Lower power consumption depending on settings and usage

Other features

- Motion-triggered wake-up and sleep timer
- Real-time clock and calendar
- Configurable command button

Figure 2-15 explains how the SmartRock monitoring system operates remotely. The system is composed of a cloud computing center which connects to the hosts – data collection systems located on the side of the track – and each host is linked to up to seven SmartRocks via Bluetooth. With remote monitoring, the SmartRocks start to collect the data and then transmit them to the hosts; afterward, the hosts will pass the data to the cloud server.

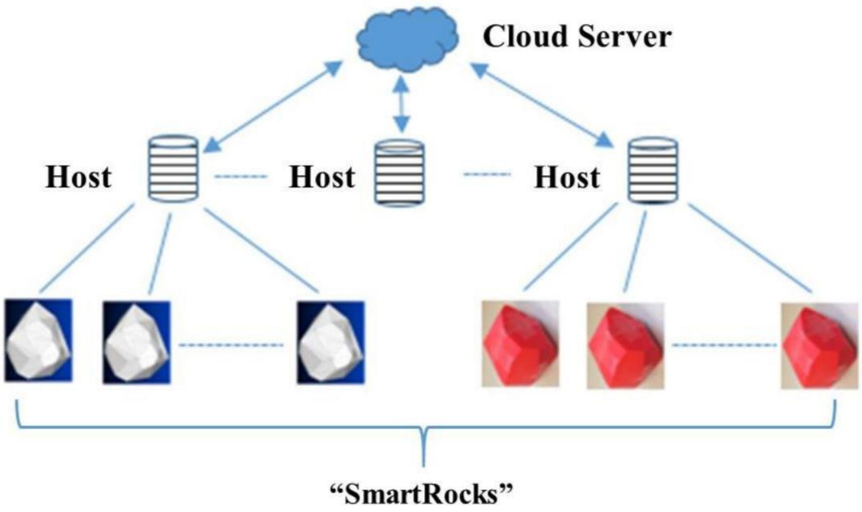

Figure 2-15: SmartRock data acquisition network(Liu, 2015)

Liu et al. (2015-2017) have conducted studies confirming the ability of the SmartRock for recording real-time rotational and translational accelerations. This capability made the possibility of monitoring the ballast particle movement in railroad engineering. In addition, ballast particles have translational as well as rotational modes under cyclic loading, both of which are proved to be important for understanding the ballast behavior based on particle movements. (Liu et al., 2017)

According to a 2015 study by Liu and colleagues (Liu et al., 2015), the authors of the study utilized the SmartRock to monitor ballast particle movement inside the ballast layer under cyclic loading. The SmartRock is beneficial for railroad ballast research because (1) it works wirelessly, and (2) its physical appearance is very close to the real ballast particle's shape in contrast to traditional accelerometers which do not share that same shape with real ballast particles. In Liu's study (Liu et al., 2015), two different approaches were employed to examine ballast particle movement: the first was DEM modeling, while the second utilized an experimental test with SmartRocks. In the DEM numerical analysis, ballast particles were simulated as uniform angular particles of one inch in diameter based on the average of No. 4 particle size distribution defined by AREMA. In the experimental test, SmartRock was buried underneath the tie in a ballast box constructed based on a half-section of a typical railroad track structure (Liu et al., 2015). Comparing the results of these two approaches, Figure 2-16 demonstrates the similar trends in the simulated and recorded motions, even though the magnitudes are different. This discrepancy can be further explained by the fact that the DEM model was not capable of reproducing the same test conditions, such as ballast placement, ballast gradation, and particle shapes. Nevertheless, the agreement in trends suggests that the SmartRock is capable of capturing the movement of individual ballast particles realistically and can therefore be used as a validation tool for DEM simulations in railroad ballast research (Liu et al., 2015).

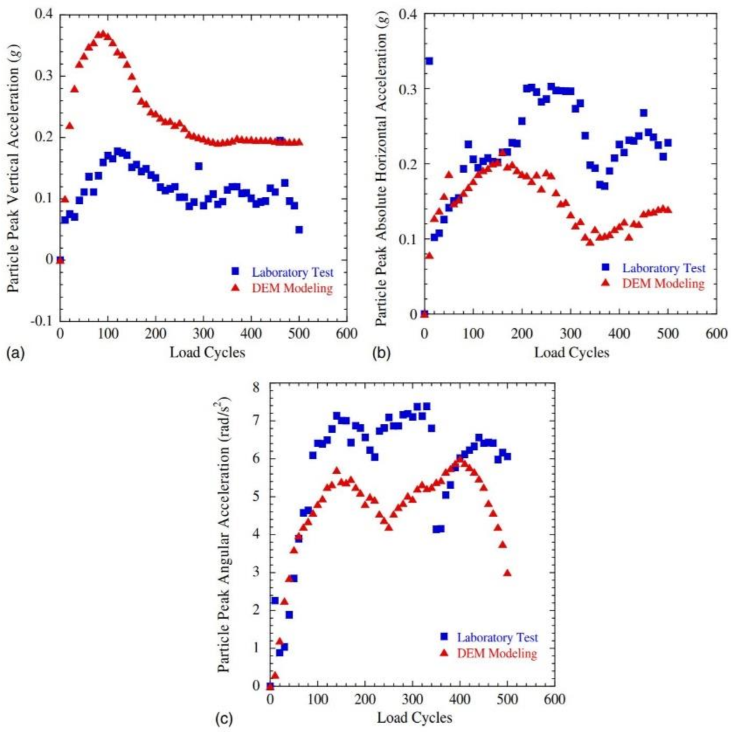

Figure 2- 16: comparison of The DEM and LAB test result: a) vertical acceleration; b) horizontal acceleration; c) angular acceleration (Liu et al., 2015)

Quantifying the advantage of utilizing geogrids in rail track bed structure to reinforce the substructure in its place has been a significant topic for researchers in recent years. One of the most current studies has been performed by Liu and colleagues (Liu et al., 2016), with the goal of investigating the impact of the geogrid on particle movement, "such as particle translational and angular accelerations, inside railroad ballast layers during initial compaction phase" (Liu et al., 2016). The experiment set consists of a ballast box containing a ballast layer, two crossties, and a rail (I-beam) which was created to simulate the structure of a half-section of railroad track. Two ballast box tests were conducted: one with a geogrid, and, for the purpose of baseline scenario, one without a geogrid. In addition, two wireless "SmartRock" devices were implanted in the ballast box, one beneath the rail seat and the other below the edge of a tie, to screen separate ballast particle movement under cyclic loading. As a result of this study, it has been concluded that "particle translational movement and rotation" are higher underneath the edge of the tie than below the rail seat, since at the incline and in hilly conditions there is less confinement which results in more vivid translational and rotational movement of particles (Liu et al., 2016).

Another result obtained in this study is that the SmartRocks installed in the ballast layer have the ability to provide kinematic information of ballast particles. Hence, the SmartRock can be considered as a potential monitoring tool because it can provide an easy, durable, and repeatable means to assess ballast behavior and performance. Regarding the effects of the geogrid on ballast particle movement, as demonstrated in Figure 2-17 the primary vertical displacement of the ballast layer for a load under 500 cycles declined significantly in the ballast box equipped with a geogrid (Liu et al., 2016).

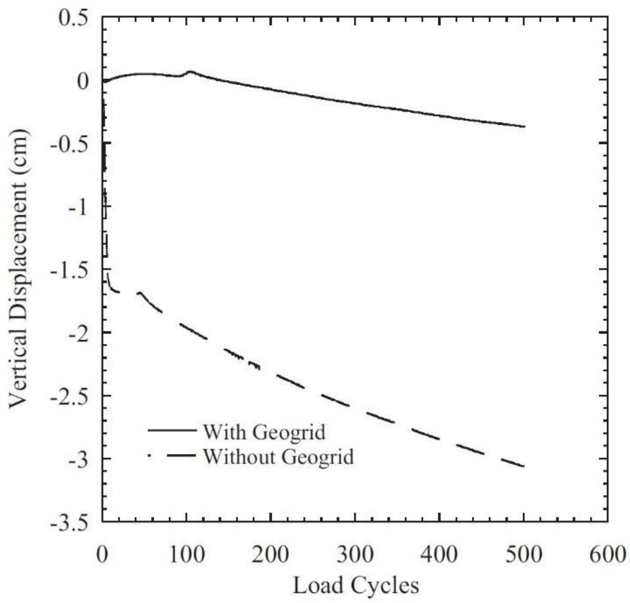

Figure 2- 17: Vertical displacement vs. load cycles (Liu et al., 2016)

So far, it has been discussed that ballast movement, comprised of translation and rotation, has an important effect on track performance. Excessive movement of ballast particles leads to track geometry unevenness, e.g., hanging ties, and thus raises the potential for damage and deterioration of rails, ties, and fastening components (Liu et al., 2017). In this regard, Liu et al. 2017 investigated ballast particle movement at different locations beneath a crosstie using SmartRock. In this study, three tests were conducted by using a ballast box which simulates a half-section of a typical railroad track. Two SmartRocks were placed beneath the middle of the tie and the edge of the tie, respectively, but at different depths during each test: directly under the tie, 12 cm beneath the tie, and 25 cm beneath the tie. Figure 2-18 schematically illustrates the test procedure. (Liu et al., 2017)

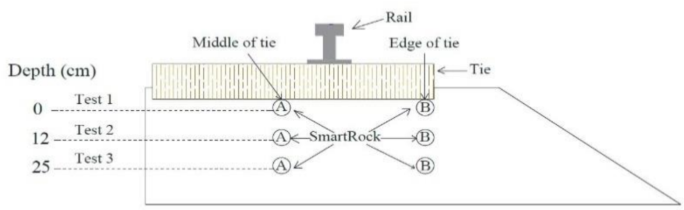

Figure 2- 18: The location of the SmartRocks in ballast box (Liu et al., 2017)

In this study (Liu et al., 2017), the effects of two parameter – position corresponding the tie and burial depth – were assessed by analyzing the recorded data of the SmartRocks at different depths in the ballast. The study determined that smart rocks were beneath the edge of the tie had higher rotation compared to those beneath the middle of the tie. ballast depth significantly reduced Particle translational movement and rotation while load cycles are fewer than 500 (Liu et al., 2017).

In 2018, Huang et al. conducted a field experiment to investigate particle movement under different ballast conditions using a battery-powered remote-monitoring system containing multiple SmartRocks. This study was conducted in an attempt to gain insight into the mechanism of mud pumping through monitoring ballast particle movement that cannot be inspected visually. The authors compared the movement pattern of ballast particle from two sections: a control section with clean ballast, and a mud-spot section with a known mud-pumping problem. Both sections were constantly observed under passenger and freight train passages and also under wet and dry ballast conditions. The statistical results of the acceleration and rotation data of ballast particles in the clean and mud-spot sections are compared in Table 2-3. According to the analysis of variance (ANOVA), the standard deviations and the ranges of acceleration and rotation were statistically different. The ranges of acceleration and rotation in the mud-spot section were over 1.5 times greater than those in the clean section. This factor can serve as an important reference value for researchers in the field who are interested in identifying abnormal ballast particle movement (Huang et al. 2018).

Table 2- 3: Statistical analysis of ballast particle movement (Huang et al. 2018)

Train Type	Acceleration (g)					Rotation (°)	
	Variable	Track Direction		Vertical Direction		Pitch	
		Mud	Clean	Mud	Clean	Mud	Clean
Freight	Mean	0.000	0.000	0.000	0.000	-0.063	-0.002
	StDev	0.023	0.010	0.022	0.016	0.088	0.034
	Max	0.502	0.150	0.354	0.411	0.375	0.091
	Min	-0.244	-0.134	-0.848	-0.403	-0.574	-0.167
	Range*	0.876	0.419	1.202	0.813	0.948	0.258
	Factor**	2.1		1.5		3.7	
Passenger	Mean	0.000	0.000	0.000	0.000	0.126	-0.003
	StDev	0.013	0.010	0.021	0.013	0.127	0.019
	Max	0.082	0.041	0.109	0.048	0.297	0.025
	Min	-0.055	-0.043	-0.100	-0.057	-0.153	-0.086
	Range*	0.136	0.084	0.209	0.105	0.450	0.111
	Factor**	1.6		2.0		4.0	

In the same study, the authors also assessed the approach to diagnosing abnormal ballast particle movements by using the Arias intensity, which measures the intensity of the ballast response and is defined as the energy dissipated per unit mass. Figure 2-19 presents the result of this approach. As seen in this figure, for the same train passage, the Arias intensity values at the mud-spot section were approximately 3.6 times greater than of the clean section based on the linear regression. For the passenger trains, the Arias Intensity values at both sections are generally small due to smaller acceleration amplitudes and shorter duration of the train passages. Under the freight trains, the Arias Intensity values are less than 1 in the clean section but can reach over 4 in the mud-spot section, suggesting lower energy dissipation and unstable ballast particles in the latter. (Huang et al. 2018)

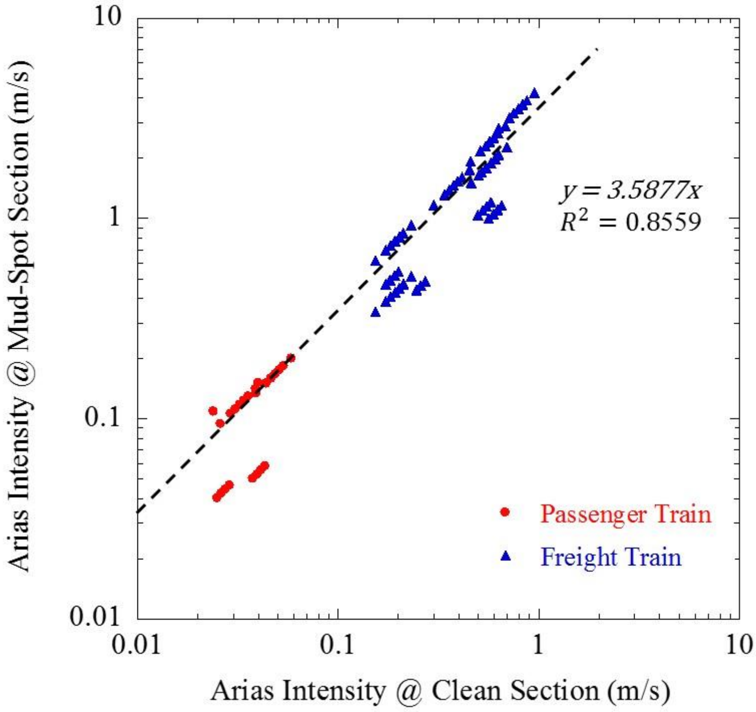

Figure 2- 19: Comparison of Arias intensity between clean and mud-spot sections (Huang et al. 2018)

3 Project descriptions

In the previous chapter, fouling is discussed as a defect in the ballast layer which adversely affects the ballast's functionality. As the top layer of track substructure that is in direct contact with superstructure components, the ballast layer is proven to have a key role in track stability and performance. Therefore, proper ballast maintenance planning is vital to ensure a safe and reliable track operation. This study has been conducted in an effort to investigate the effects of fouling in particle movements recorded using the SmartRock, with a further step providing an algorithm to detect the fouling from the SmartRock data. For this purpose, two sections with similar traffic but different track conditions, one with clean ballast and the other with mud pumping, were chosen in an under-operation track. Several SmartRocks were installed in both sections and a set of real field experiments were conducted. The SmartRock was placed in a crib and also in the shoulder part of the ballast; data representing the ballast particle rotational and translational movement were collected both for freight and passenger train over a span of one week. In the following sections, the characterization of the site and the detailed instrumentation are discussed.

3.2 Site Selection

In this study, two test sections, one clean and one mud-spot, of a ballasted track with wood ties located in Bellwood, Pennsylvania were chosen. In this track, despite regular maintenance, mud pumping at this section is a recurring problem.

The two chosen sections are located in close distance on the same tangent track; they are considered identical in terms of the traffic load and environmental conditions (Huang et al., 2018).

Figure 3-20 provides a comparison of the clean section and the mud-spot section. There is a severe mud pumping appears to be visible in Figure 3-20 (b). In the preliminary visual inspection of the mud-spot section, several observations were made during the field instrumentation installation. ponded water is noticeable underneath the tie and as a result, the ballast is completely penetrated by subgrade materials. Beside the mud pumping area, a gap was found to exist at the tie-ballast interface and the ties were poorly supported. Additionally, in some areas, the problematic ties were hanging on the ballast; these ties create high dynamic forces upon wheel load (Huang et al., 2018).

Figure3- 20: Comparison of two sections: (a) clean section; (b) mud-spot section (Huang et al, 2018)

3.3 Instrumentation plan

Similar instrumentation was used in both sections to provide real-time data processing and viewing. A wireless system powered by a battery was utilized to automatically collect data and transfer that data remotely. This system consisted of multiple devices including SmartRocks, a data acquisition system, a Wi-Fi hotspot, an antenna, a remote monitoring device, a solar panel and DAQ box for a storage battery, and a power inverter. The SmartRock monitoring system is fully illustrated in Figure 3-21 (Huang et al., 2018).

As illustrated in this Figure, the DAQ box in the SmartRock monitoring system works as a trackside “host” to communicate with the SmartRocks. It is worth mentioning that this monitoring system is set up for remote operation. The remote monitoring device empowers the SmartRocks to start collecting and transmitting data. Next, the hosts will pass the SmartRock data to a cloud-based computer center using Wi-Fi. The power management system at the SmartRock node level allows the SmartRocks to sleep between readings to save battery life (Huang et al., 2018).

Figure 3- 21: A photo of instrumentation: (a) SmartRocks and ballast particles; (b) illustration of SmartRock monitoring system (Huang et al., 2018)

As Figure 3-22(b) indicates, five SmartRocks were mounted underneath the tie and in the crib 10 cm below the ballast surface in each section to capture and compare the particle movement under train passages. In this study the data collected from both freight trains (around 40 km/h), with an average axle load of 32,000 kg, and passenger trains (AMTRAK) (around 115 km/h), with an average axle load of 16,150 kg (Huang et al., 2018).

During the installation process the following procedure happened:

- The ballast was excavated by shovel
- The SmartRocks were located at the desired locations
- The ballast was filled and compacted by an electric jackhammer

The field installation was planned in such a way that it took a minimum amount of time (installation in one hour) and crew without requiring heavy machinery or dismantling the track. Despite the partial removal of the ballast, train operations continued. No rail compaction was needed because no major excavation was conducted. In addition, the installation did not disrupt train traffic because the subject area has busy traffic with a train passage approximately every half-hour. After the installation of the SmartRocks, the performance of the data acquisition system was evaluated for three days prior to the commencement of data collection (Huang et al., 2018).

Figure 3-22: Instrumentation installation: (a) internal measurement unit mounted on tie; (b) SmartRocks installed in crib (Huang et al., 2018)

4. Data analysis and results

Maintenance of the railway track is crucial for a safe and reliable track operation. The frequent inspection of track components using various technologies generates a huge amount of data. extracting the information regarding the track condition from this data has been considered as a challenge for researchers. Generally, the maintenance approaches in railway can be classified into three categories. The first approach is corrective maintenance, which involves waiting until failures occur and performing maintenance in order to fix the problem; this approach is expensive and involves unexpected service interruptions, which makes it inefficient. The second approach is preventive maintenance, in which the maintenance task is planned regularly based on certain criteria in order to prevent failure from happening. In this approach, the maintenance is scheduled in specific intervals. Therefore, the advantage is that the time of service interruption is predictable, but on the other side there is a possibility of replacing a part before it becomes inoperative. condition-based maintenance is the third approach that becomes possible by using real-time analysis of the data generated from inspection technologies. In this approach, the future condition of the asset can be predicted. Moreover, as a result of continuous monitoring of the asset, maintenance tasks are performed as soon as the potential for degradation is detected. (Ghofrani, 2018)

This study aimed to develop an algorithm for real-time evaluation of the ballast condition using the translational and rotational particle movement data collected by SmartRocks. The SmartRocks were installed within the ballast layer and the data was acquired by monitoring the two track sections — one clean section and the other the mud spot — over a period of one week. Figure 4-23 illustrates the direction of the acceleration and rotation recorded by the SmartRocks. The translational acceleration is recorded in three directions: vertical, in alignment with track, and also in tie direction. Yaw, roll, and pitch are the directions of the rotational movements (Huang et al., 2018).

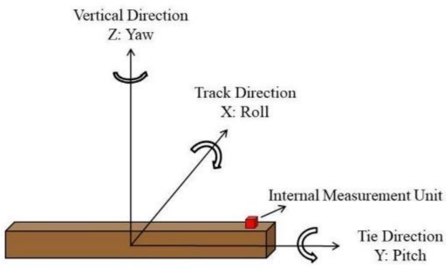

Figure 4- 23: Convention direction for SmartRock ((Huang et al. 2018)

in following figures, the raw time histories data obtained from the SmartRocks placed in the crib ballast are plotted to gain some initial insight into the signal. These time histories were recorded with the sampling interval of 0.016 seconds. The red color represents the data from the mod spot and the blue refers to the clean ballast data.

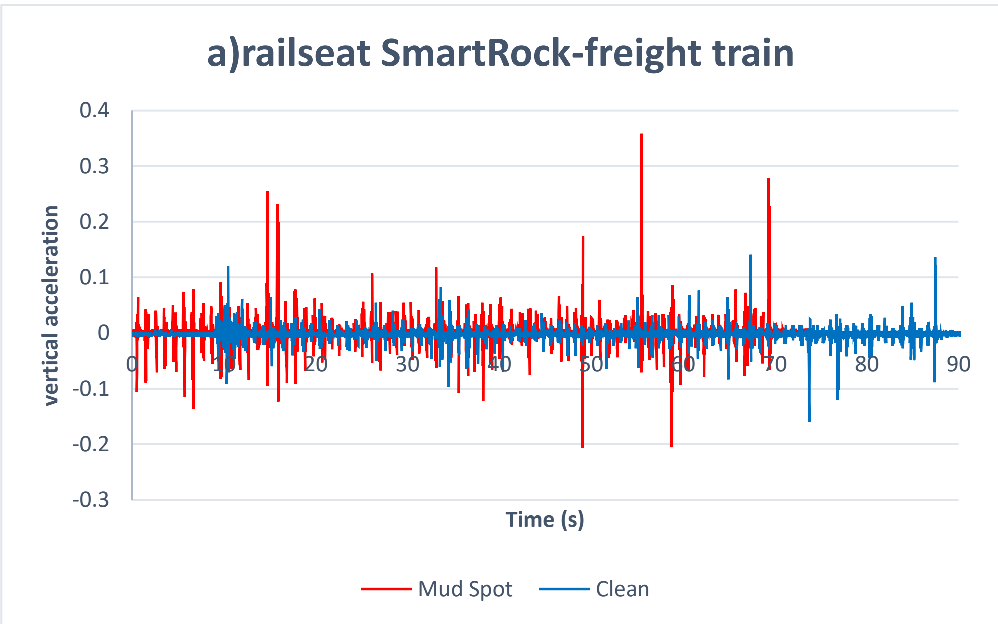

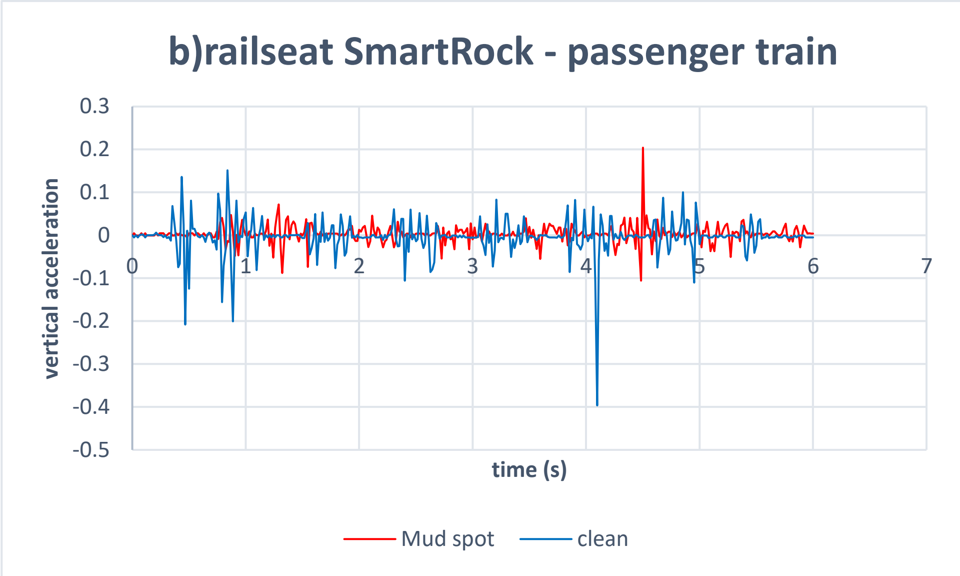
b)railseat SmartRock - passenger train
0.3
0.2
0.1
0
-0.1
-0.2
-0.3
-0.4
-0.5
vertical acceleration
0
1
2
3
4
5
6
7
time (s)
Mud spot
clean

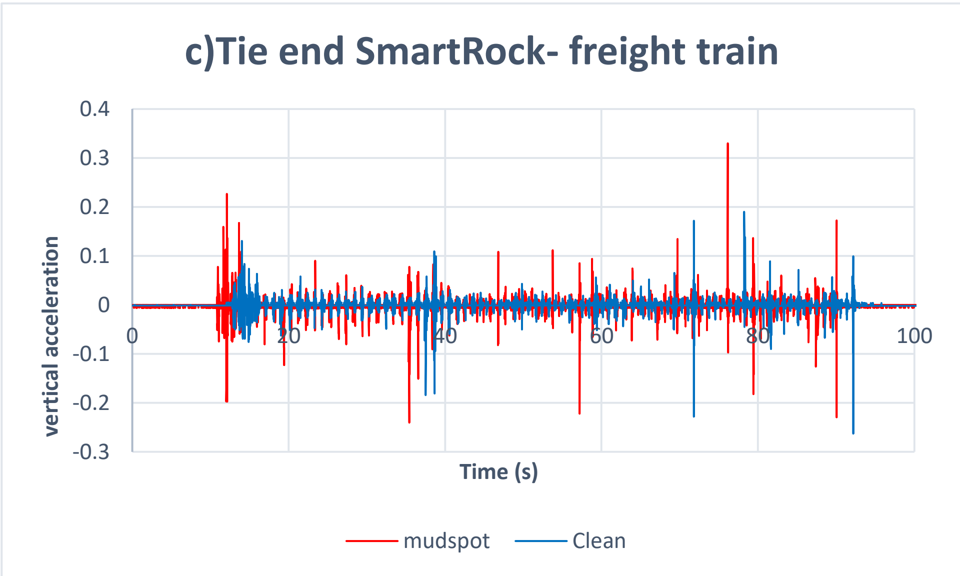
c)Tie end SmartRock- freight train
0.4
0.3
0.2
0.1
0
-0.1
-0.2
-0.3
vertical acceleration
0
20
40
60
80
100
Time (s)
mudspot
Clean

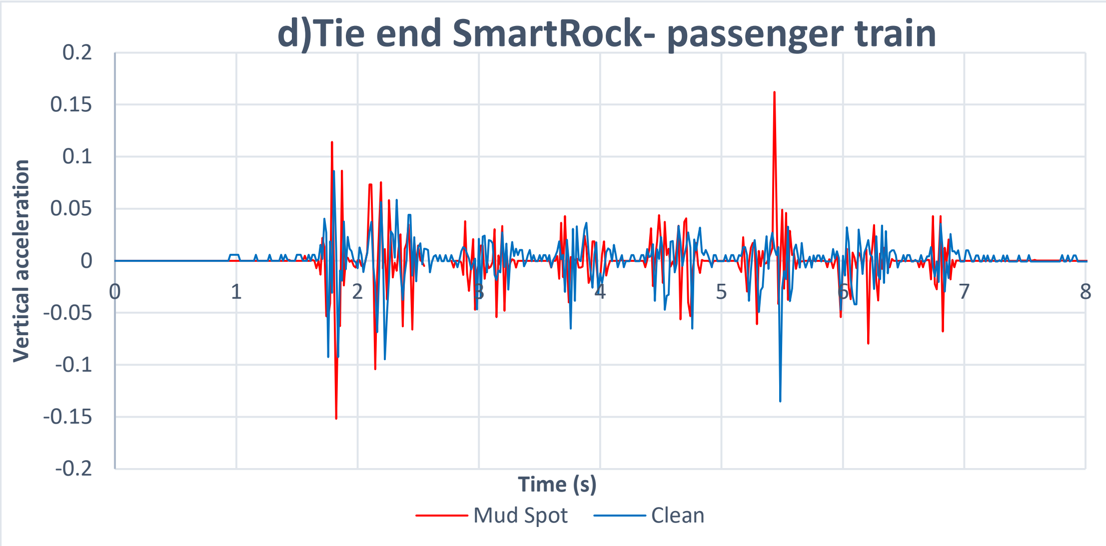

Figure 4-24: The vertical acceleration recorded from the SmartRock in shoulder ballast: a) in the railseat under freight train load; b) in the railseat under passenger train load; c) at the end of the tie under freight train load; d) at the end of the tie under passenger train loading

Based on these plots, no consistent trend (upward or downward) in ballast particle movements over the entire span of the time has been found. Comparing the data from two different sections reveals that in the mud spot area, the SmartRocks experienced higher peak vertical acceleration, especially under freight train load.

In the plotted raw time series, three various patterns are recognizable in the recorded acceleration, including “the group effect of four closely-spaced wheels, impulse-like peak accelerations caused by dynamic impact from the wheel load and small or no accelerations from the middle of each car”. (Huang et al., 2018)

In pre-processing the data as the preliminary step, each group effect was considered as a time window in further analysis. Moreover, since in a train set the weight of each car is different, each group effect scaled between -1 to 1.

Based on the previously mentioned studies in the literature of this study, four-step SHM procedure consists of “operational evaluation, data acquisition and cleansing, feature selection, and statistical model development” (Sohn et al., 2001).

In this study, since each time window consisted of the data collected over a few seconds, the environmental like temperature could be considered as constant. Therefore, in operational evaluation step, it was assumed that the variation caused by environmental and operational condition change was negligible. These considerations led to the decision not to normalize the data and focus on feature extraction and statistical modeling for feature discrimination.

Feature extraction is the process in which an attribute that is sensitive to the damage is identified. A feature should be defined and examined to separate these data because recognizing whether data was collected from a damaged or undamaged structural condition is often difficult by data visualization alone (Sohn et al., 2002). One of the most common approaches in time series data for feature selection is to use the autoregressive (AR) model, also referred to as linear predictive coding (LPC) (Farrar et al., 1999).

In this study, the vertical acceleration from the SmartRocks in the crib ballast was used and the AR model was built for each group effect; the coefficients of AR models were then selected as damage-sensitive features. Prior to applying the AR model, all the signals were standardized by subtracting the mean from individual data and next dividing by the standard deviation. This standardization procedure was applied to all signals used in this study so that the data would be rescaled to a dataset with a mean of zero and a standard deviation of one. The AR model tries to predict one variable using a linear combination of past values of the variable. In the AR(n) model, "n" is the order of the regression which represents the number of previous data points used to model the current data point. The equation below presents the general definition of a "p" order AR model (Sohn et al. 2000)

$$Y(t) = \sum_{j=1}^{p} \varphi_j Y(t-j) + e_t \qquad 10$$

where y(t) = is the measured data at time t; φ_j is unknown AR coefficient and e(t) is the random error.

The partial autocorrelation function (PACF) is used to define the most efficient order of the AR. In time series data, the PACF defines the partial correlation of a single value with its own lagged values when removing the effect of the other values in between these two lags (Gul, 2009). If the AR model is appropriate for the data, the PACF plot should cut off after p lags and the P^{th} lag is the most significant lag that will be used for making the prediction.

The PACF plot of the data recorded by the SmartRocks in the rail seat and also in the tie end area under the passenger train is provided in Figure 4-25. Examining these PACF plots, it can be seen that the correlation of the third lag is significant in both plots and the following lags are not significant. It can be concluded that there was an autoregressive term in the data, and also that the third order is the best for the AR model. Therefore, a third order AR model was applied on vertical acceleration signals recorded by the SmartRocks in the crib part.

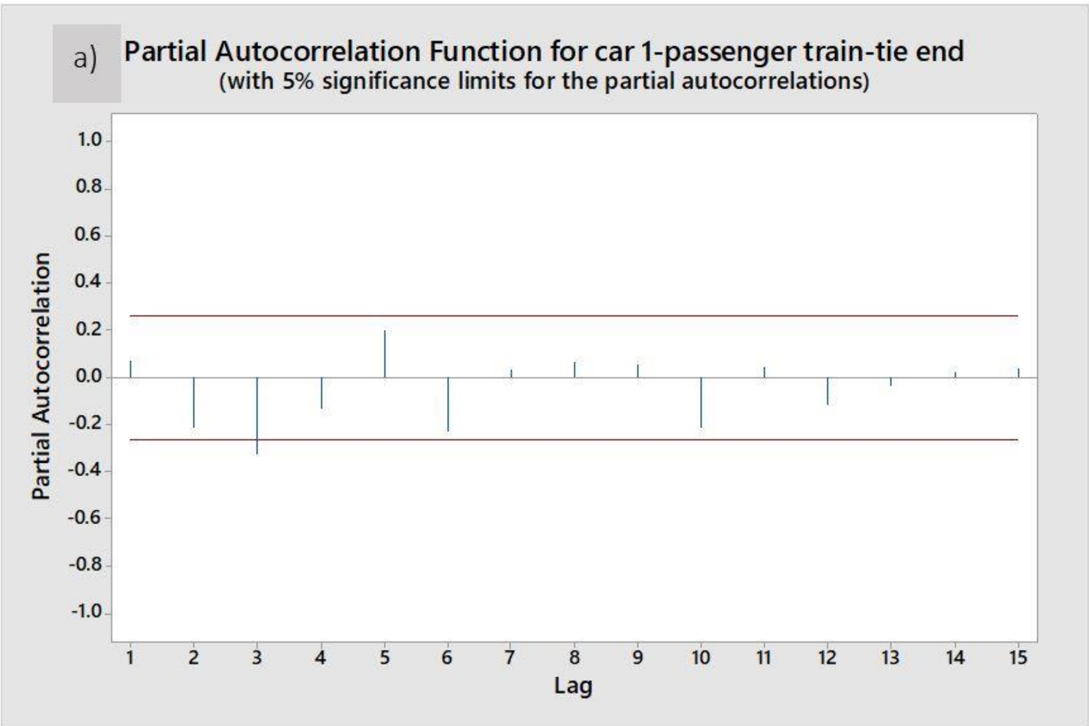

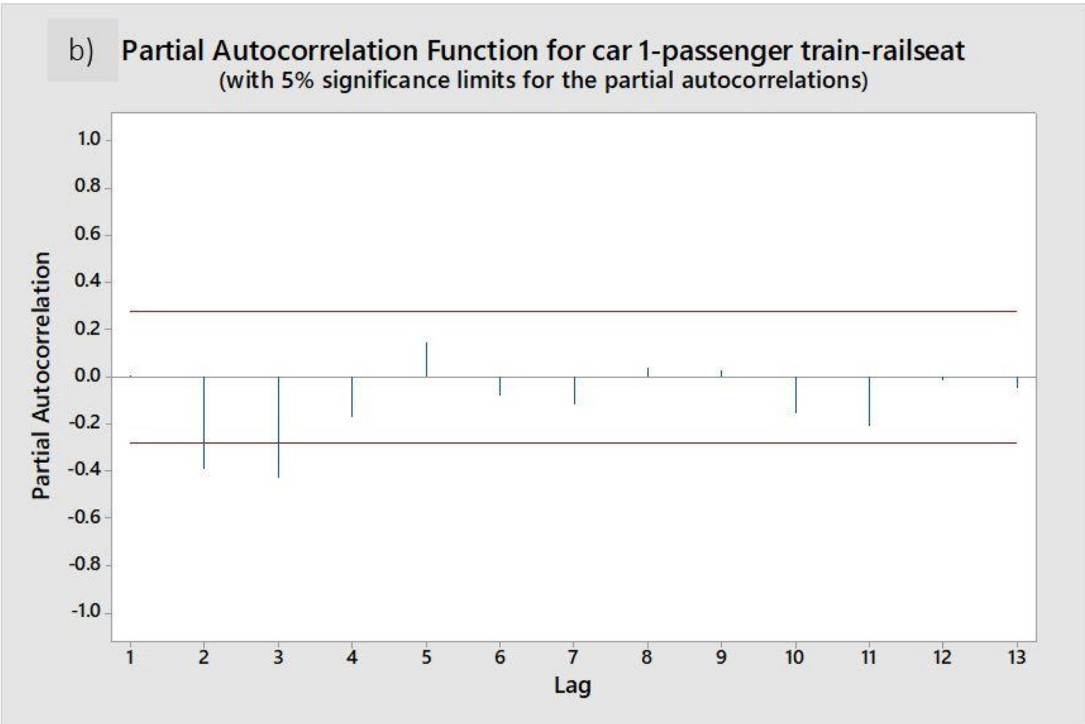

Figure 4-25: The partial autocorrelation function plot for the first car a) tie end SmartRock and b) railseat SmartRock

Statistical model development is related to developing the algorithms and applying them to the obtained features to define the structural condition of the monitored structure. “Group classification, regression analysis, and outlier detection” are the common approaches for damage detection processes (Sohn, 2001).

This study proposed two different methods based on the statistical analysis of the measured data so as to investigate how mud pumping affects the ballast layer in terms of particle movement. The first approach is the statistical chart control for the outlier detection and the second is the classification by linear discriminant analysis.

a) Statistical control chart

When it comes to the continuous monitoring of a structure, control charts are among the most popular outlier detection approaches for damage detection. After identifying the damage-sensitive features, any damage that occurs in the system is expected to change the mean or the variation of these features. Therefore, using the control chart makes it possible to distinguish the inconsistency in the new data comparing to the past data (Sohn et al. 2000).

In this study, a X-bar chart is used, after extracting the sensitive feature by fitting the AR model, for the anomaly detection. The X-bar chart includes three control lines, the central line (CL), the upper control line (UCL), and the lower control line (LCL), in order to track any abnormal changes in the data (Sohn et al. 2000). The centerline is the mean of the extracted features and two control limits is defined by setting a = 0.01 in the following equation (Sohn et al. 2000):

$$UCL, LCL = CL \pm T\alpha_{/2} \frac{S}{\sqrt{n}} \qquad 11$$

The features are standardized prior to plotting them in the control chart. Control charts generally assume that the data distribution is normal, but it has been proven that defining control limits works also if the features is not exactly normal (Sohn, 2000).

In this study, we had two sets of features obtained from the reference data and the mud spot. The control limits were defined based on features of the clean section, and the AR coefficients of the mud-spot section were then evaluated relative to the previously defined control limits. From the statistical viewpoint, those features that are outside the control limits in the control charts are referred to as outliers, and a substantial number of outliers indicates that the system is experiencing damage (Sohn et al. 2000).

In this study, the coefficients of the third order AR model were defined as damage indicator attributes and were used in the following control chart analysis. In Figure 4-26, AR coefficients extracted from individual measurements of the ballast particles' vertical acceleration are plotted in the X-bar control chart. The data utilized in the control chart are from the SmartRock placed in crib ballast in two areas; at the tie end and the railseat.

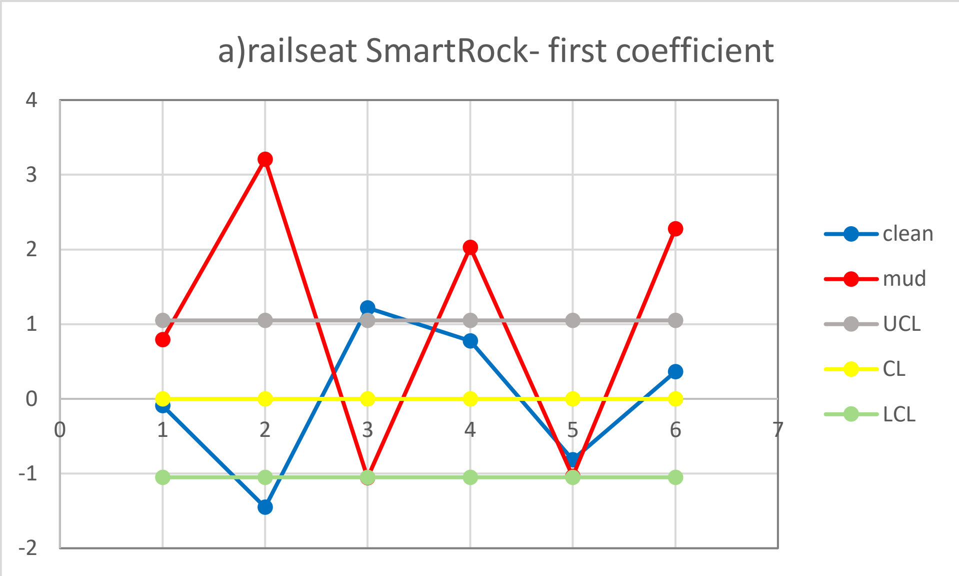
a)railseat SmartRock- first coefficient
4
3
2
1
0
-1
-2
0
1
2
3
4
5
6
7
clean
mud
UCL
CL
LCL

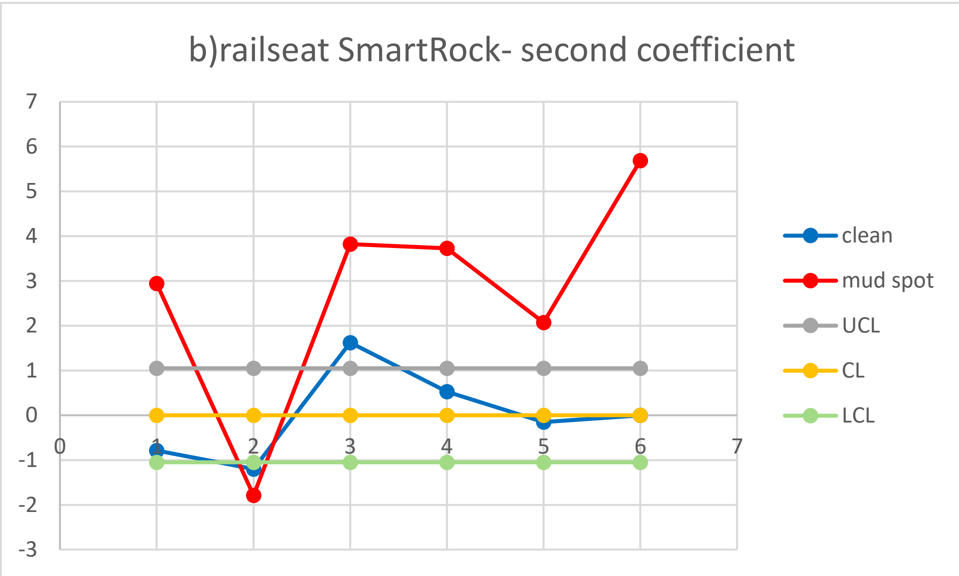
b)railseat SmartRock- second coefficient
7
6
5
4
3
2
1
0
-1
-2
-3
0
1
2
3
4
5
6
7
clean
mud spot
UCL
CL
LCL

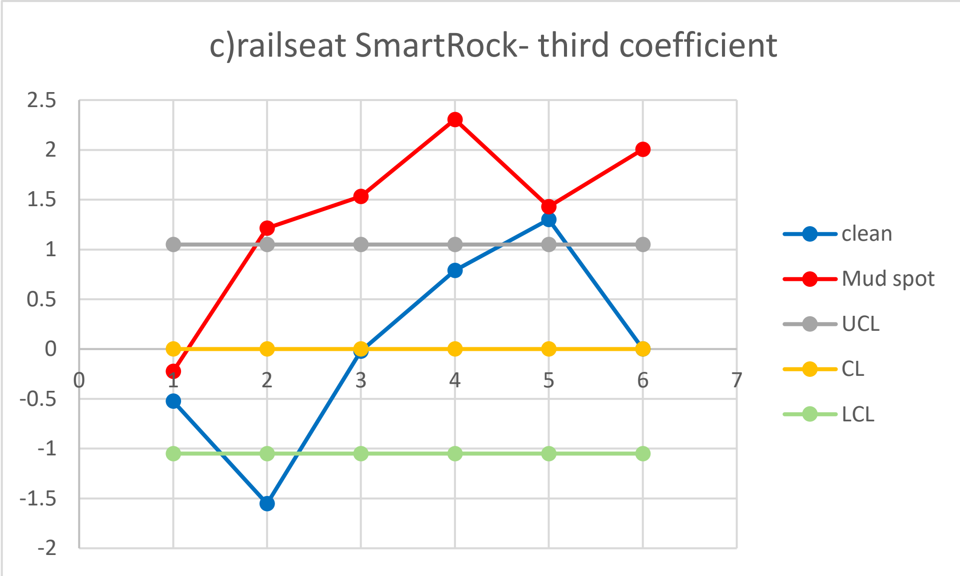
c)railseat SmartRock- third coefficient
2.5
2
1.5
1
0.5
0
-0.5
-1
-1.5
-2
0
1
2
3
4
5
6
7
clean
Mud spot
UCL
CL
LCL

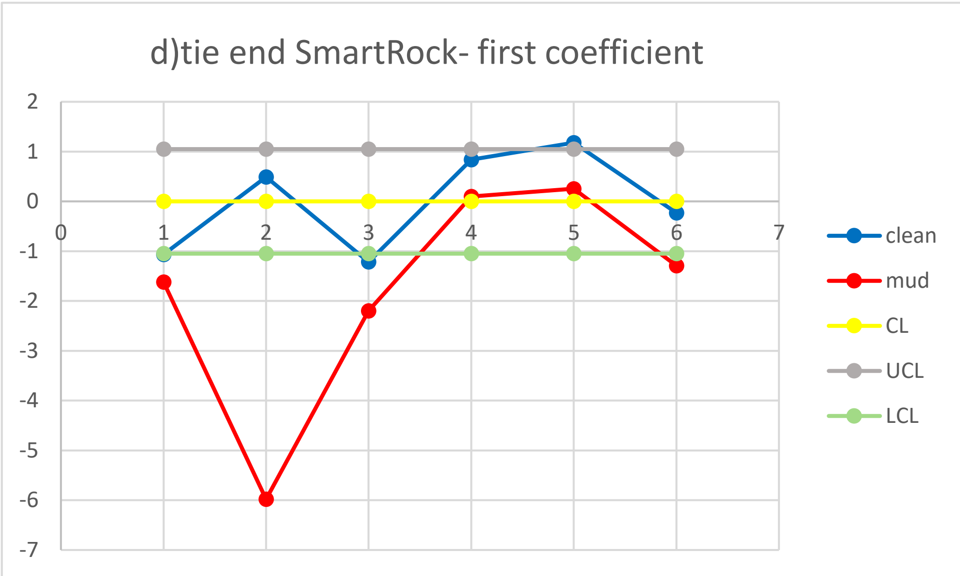
d)tie end SmartRock- first coefficient
2
1
0
-1
-2
-3
-4
-5
-6
-7
0
1
2
3
4
5
6
7
clean
mud
CL
UCL
LCL

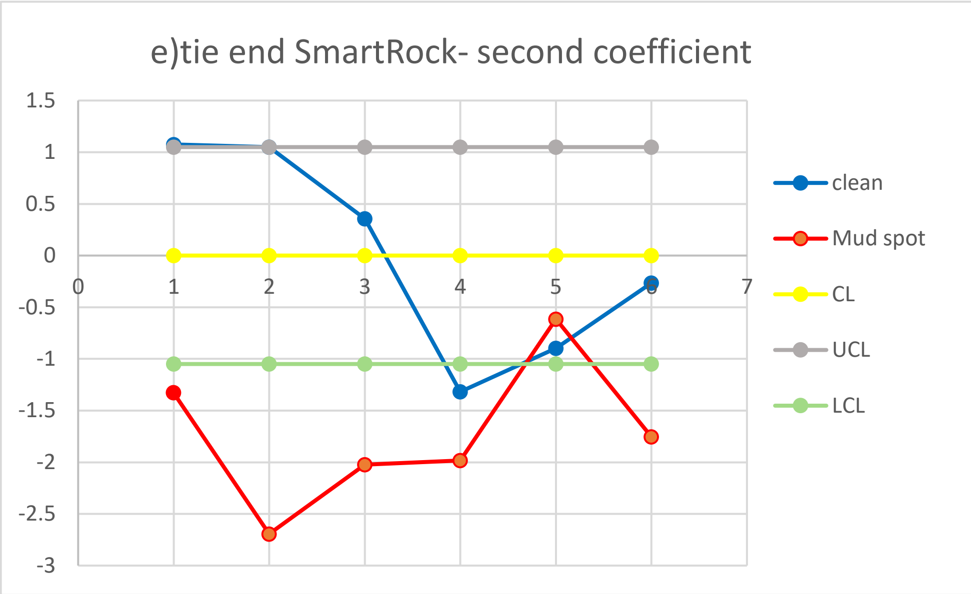

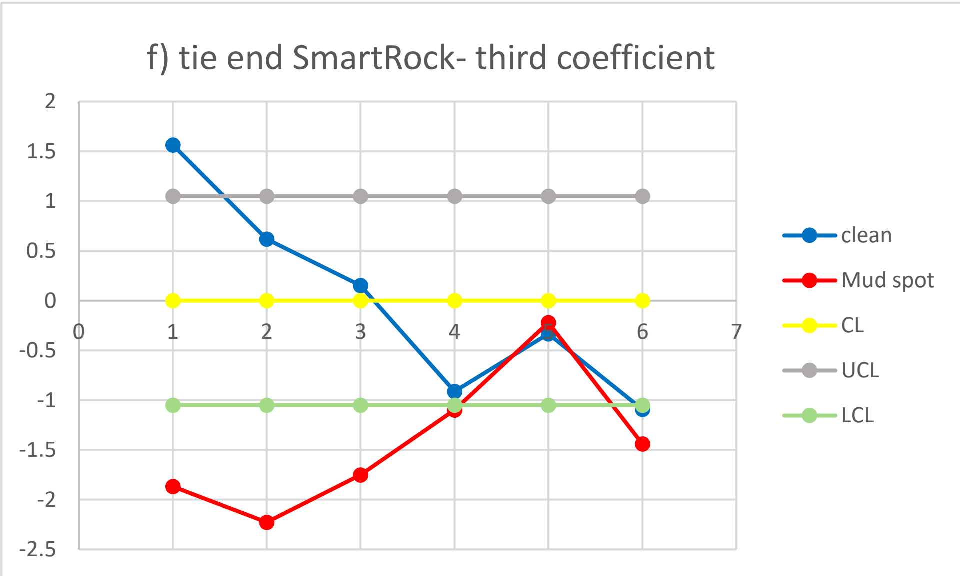

Figure 4-26: X-bar control chart with clean and mud-spot data AR coefficients in order to facilitate outlier detection; a) railseat, first coefficient; b) railseat, second coefficient; c) railseat, third coefficient; d) tie end, first coefficient; e) tie end, second coefficient; f) tie end, third coefficient

Table 4- 4: Summary of the number of outliers in the X-bar control chart for the tie end and rail seat SmartRock

	Tie end		rail seat	
AR coefficient	Clean section	Mud spot	Clean section	Mud spot
A1	0/6	3/6 (50%)	2/6	3/6 (50%)
A2	1/6	5/6 (83%)	1/6	5/6 (83%)
A3	1/6	4/6 (83%)	2/6	5/6 (67%)

The measured vertical acceleration for the passenger train included six group effects; applying AR (3) to each of them resulted in six sets of AR coefficients. Figure 4-26 displays the anomaly detection results using each coefficient of the AR (3) model in the X-bar chart control.

In the X-bar chart, upper and lower control limits and centerline were represented by UCL, LCL, and CL sign, respectively. The control limits and the center line correspond to the 99% confidence interval and mean of the data (Sohn et al. 2000). These control limits were constructed from the time series data collected from the reference section with clean ballast. The standardization process was performed on the features prior to plotting the control chart by subtracting the mean and dividing by the standard deviation of the feature (Sohn et al. 2000). Therefore, the CL in all of the previously mentioned X-bar charts is equal to zero. After establishing the control limits and centerline, features obtained from the mud-spot data were plotted relative to the control limits and centerline obtained from the reference data (Sohn et al. 2000).

Table 4-4 summarizes the results of the damage diagnosis using the AR coefficients. From these results, evident outliers can be seen in the mud spot features. Moreover, it can be determined that the second AR coefficient is more indicative in term of damage, while the first coefficient is less sensitive to damage.

b) LDA classification

In this section, the vertical acceleration data from the SmartRocks in the crib ballast are analyzed using the linear discriminant technique. The linear discriminant analysis (LDA), also known as "Fisher's Discriminant", is a classification algorithm introduced in the literature of this study as one of the approaches used for the structural anomaly detection. Generally, the classification methods are among the supervised learning approaches that need data from both structural conditions available while in the outlier detection, the algorithm can be developed with just the reference data (Farrar, 1999).

LDA tries to determine the best linear classifier and achieve the most separability between various classes in the feature space. To that end, the LDA algorithm tries to apply hyperplane projection in a way that, for the projected data, the between-class mean is maximized and the variance of the within-class data minimized (welling, 2005). Figure 4-27 schematically depicts how the LDA separates the classes of the data by finding a linear combination of the features.

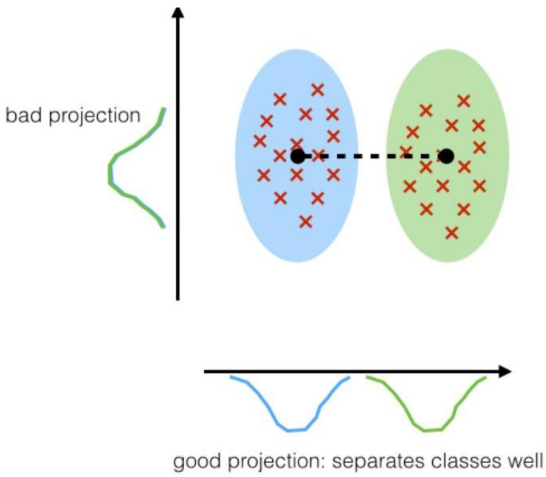

Figure 4-27: LDA projection

(from http://sebastianraschka.com/Articles/2014_python_lda.html)

The LDA initial concept is to classify the data by projecting the feature space in a direction that maximizes the separation of different classes (Bishop, 2006). For algorithm of the LDA (Bishop, 2006), first assume a set of observation (x) with two classes of data. The mean of each class is $\vec{\mu}_1$ and $\vec{\mu}_2$. Assume $\vec{\omega}$ as the matrix project the x data into scalar y as follows:

$$y = w^T x \tag{12}$$

the projected features would have a mean equal to $\vec{\omega}.\mu_i$. In order to define the separation of linear classifies between these 2 classes of data through LDA, the ratio of the variance between the classes to the variance within the classes should be calculated with the following equation

$$\mathrm{F}\{\mathrm{w}\} = \frac{(\mu_1 - \mu_2)^2}{S_1^2 + S_2^2} \tag{13}$$

Which $S_i$is the within class variance of the projected data is calculated using the equation below:

$$S_i^2 = \sum(y_n - \mu_i)^2 \tag{14}$$

This equation based on the W can be written as follows:

$$F\{w\} = \frac{w^T S_B w}{w^T S_w w} \qquad 15$$

In this equation;

S_B is the between class covariance matrix as

$$S_B = (\mu_1 - \mu_2)(\mu_1 - \mu_2)^T \qquad 16$$

And S_w is the within class covariance matrix as:

$$S_w = \sum(X_n - \mu_2)(X_n - \mu_2)^T + \sum(X_n - \mu_1)(X_n - \mu_1)^T \qquad 17$$

Furthermore, it can be demonstrated that with the maximum separation proper $\vec{\omega}$ is proportional to:

$$\vec{\omega} \propto {S_w}^{-1}.(\mu_1 - \mu_0) \qquad 18$$

In this classification method, the response variable should be categorical, and this algorithm attempts to assign an individual observation to one of the categories in the response variable. Generally, for building a classification model, a set of training data is needed. The classifier will be defined based on these training data; the model performance will subsequently be evaluated by applying the algorithm to a new set of data (called test data) and predicting the class of each individual observation in test data. Finally, the accuracy of the model can be determined by comparing these predicted class and the true class of test data.

In this study, the features extracted from the vertical acceleration data for both tie end area and rail seat were standardized in the first step prior to any subsequent analysis. The mean and the standard deviation of the features are zero and one, respectively. Afterward, through random selection, 70% of the features were selected as the training data and the remaining 30% considered as the test data. The model was initially fitted on the training data set and then applied to the test set in order to evaluate the accuracy of the model. The LDA was applied to the extracted AR coefficients and the results are provided in Table 4-5. By constructing a confusion matrix, it is possible to compare the LDA predictions and the true classes and define the type of errors in prediction.

Table 4- 5: The confusion matrix of LDA on extracted features a) at tie end, both freight and passenger train; b) at rail seat, both freight and passenger train; c) at tie end, just passenger train data; d) at Rail seat, just passenger train data

a)

Tie end	Clean	Mud	Total
True	34	24	58
Prediction	19	39	58

b)

Rail Seat	Clean	Mud	Total
True	28	27	55
Prediction	33	22	55

c)

Tie end	Clean	Mud	Total
True	4	3	7
Prediction	3	4	7

d)

Rail Seat	Clean	Mud	Total
True	4	4	8
Prediction	7	1	8

Considering the confusion matrixes above, combining the features from the freight train and passenger train for the rail seat SmartRock, the LDA model resulted in 67.1% accuracy, while for the tie end SmartRock the accuracy of the model was 45.48%. Proceeding with the model, with only the passenger train, features resulted in 74% and 55% accuracy for the tie end and rail seat, respectively.

5. Conclusions and recommendations

This research focused on developing an approach to identify the mud spot by using advanced sensor networks and statistical analysis. SmartRock is a battery-powered remote sensor that can provide insight into the ballast structural condition by capturing the movement characteristics of ballast particles. The ballast layer is responsible for providing support and drainage for the superstructure components. In this regard, ballast can be considered as the component that plays the most vital role in maintaining track stability. Ballast consists of aggregate particles and its particle size distribution is one of the most important properties that define ballast behavior. Fouling is one of the ballast defects and occurs as a result of particle breakage, or shipping of fine particles from outside the track. The fouled ballast loses the ability to function properly and maintenance actions become necessary to maintain the efficiency and safety of track operation. Therefore, monitoring the ballast condition is a crucial measure that should be taken to guarantee a safe and reliable track performance. For this purpose, statistical pattern recognition techniques were proposed in this research in order to design an algorithm that can analyze the rotational and translational movement of ballast particles recorded using SmartRocks and ultimately distinguish between data from a mud spot and that from a clean ballast. In the field experiment, data were collected from two different sections of a ballasted track with identical traffic and environmental conditions but one with clean and the other muddy ballast. Two types of algorithms were applied to the data: first, the statistical control chart for outlier detection, and second, the LDA for classification of the data. Important findings and recommendations for future research are summarized in the following sections.

5.1 Conclusion

Many studies have been conducted on structural health monitoring utilized statistical pattern recognition techniques for damage detection (Farrar, 1999). This research sought to develop an algorithm to distinguish the SmartRock data from different ballast structural conditions. The analysis of the previously-mentioned field experiment has led to following conclusions:

1. The initial visualization of data indicates that in the vertical acceleration recorded by the SmartRocks embedded in the crib ballast, the particles in the mud spot experienced higher peak vertical acceleration comparing to those in clean ballast.
2. Based on the PACF results, it was discovered that there is an autoregressive term in the data, and also that the third lag is the most significant term in the AR model. Therefore, a third order AR was applied to the data and the autoregressive coefficients were chosen as the damage-sensitive features.
3. Statistical control charts are considered one of the outlier detection approaches that are suitable for continuous monitoring. Applying this approach to the passenger train data from the crib ballast, the features extracted from the mud spot indicated obvious outliers. Among the AR coefficients, the second coefficient was revealed to be more sensitive regarding the damage detection while the first coefficient was the least sensitive one.
4. In the linear classification algorithm development, the data was divided into groups of training and test data. Following to the training the algorithm, the evaluation of its accuracy using the test data indicated that the model considering

only the passenger train features resulted in 74% and 55% accuracy for the tie end and rail seat, respectively. Combining the features from the freight train and passenger train, the LDA model for the SmartRock placed in the railseat resulted in 67.1% accuracy and for the tie end SmartRock the accuracy of the model was 45.48%.

5.2 Future recommendations

The conclusions drawn from this research study regarding the development of an algorithm for ballast damage detection is only the beginning for an improved understanding of ballast behavior. The recommended future research areas are as follows:

1. The SmartRock is a sensor that resembles a real ballast particle in terms of shape and other physical properties such as specific gravity. This sensor was developed in order to record ballast particle rotation, translation, and orientation. The SmartRock features various work modes including reset, sleep, and wake-on-motion. Currently, the change between these modes should be done manually. In order to introduce the SmartRock as a sensor for continuous monitoring of the ballast condition, further studies should be done in order to enable the sensor to be fully automatic.

2. Additional field experiments are needed to collect more data and improve the data set to be able to develop more accurate and valid results. In order to develop a comprehensive algorithm to work jointly with the SmartRock sensor as a ballast condition monitoring system a comprehensive data set including data from various ballast conditions and levels of fouling are required. Moreover, for obtaining more accurate result the algorithm should account for environmental and operational variability such as temperature.

3. In further studies, other statistical analysis approaches should be examined in order to determine the most efficient approach that works with the data. Moreover, by having data from various environmental and operational conditions, conducting data normalization will enable the development of a more comprehensive algorithm.

developing a ballast monitoring system called “ballast real-time information system (BRIS)” is the ultimate objective of this research. Future studies should be conducted in a direction to achieve this goal. This system is considered to be able to detect ballast defects which is not recognizable visually (usually early stage) and predict the future ballast condition.to this end when the train is passing SmartRocks start to collect the data. Afterward, the data will be passed to a cloud computing center wirelessly. The cloud computing is where the damage detection algorithms will be applied to the data in order to examine the ballast condition and indicate the risk of damage or failure in ballast. Hereby, BRIS is expected to greatly enhance rail operation safety and maintenance planning efficiency.

References

[1] Balakrishnama, Suresh, and Aravind Ganapathiraju. "Linear discriminant analysis-a brief tutorial." *Institute for Signal and information Processing* 18 (1998): 1-8.

[2] Brownjohn, James MW. "Structural health monitoring of civil infrastructure." *Philosophical Transactions of the Royal Society of London A: Mathematical, Physical and Engineering Sciences* 365, no. 1851 (2007): 589-622.

[3] Camargo, Luis Fernando Molina, J. Riley Edwards, and Christopher PL Barkan. "Emerging condition monitoring technologies for railway track components and special trackwork." In *2011 Joint Rail Conference*, pp. 151-158. American Society of Mechanical Engineers, 2011

[4] Christopher M. Bishop. 2006. Pattern Recognition and Machine Learning (Information Science and Statistics). Springer-Verlag New York, Inc., Secaucus, NJ, USA.

[5] CN (Canadian National) Rail. Ballast performance in concrete tie track. Prairie region. Edmonton. CN, Geotechnical Service. Internal report; 1987.

[6] Farrar, Charles R., David A. Nix, Thomas A. Duffey, Phillip J. Cornwell, and Gerard C. Pardoen. Damage *identification with linear discriminant operators*. No. LA-UR-98-4702. Los Alamos National Lab., NM (US), 1999.

[7] Farrar, Charles R., Thomas A. Duffey, Scott W. Doebling, and David A. Nix. "A statistical pattern recognition paradigm for vibration-based structural health monitoring." *Structural Health Monitoring* 2000 (1999): 764-773.

[8] Farrar, C. R., and Doebling, S. W. (1999). "Vibration-Based Structural Damage Identification," accepted for publication of Philosophical Transactions: Mathematical, Physical and Engineering Sciences, Royal Society, London, UK..

[9] Feldman, Frank, and Darryl Nissen. "Alternative testing method for the measurement of ballast fouling: percentage void contamination." *CORE 2002: Cost efficient railways through engineering* (2002): 101.

[10] Ghofrani, Faeze, Qing He, Rob MP Goverde, and Xiang Liu. "Recent applications of big data analytics in railway transportation systems: A survey." *Transportation Research Part C: Emerging Technologies* 90 (2018): 226-246.

[11] Gul, Mustafa, and F. Necati Catbas. "Statistical pattern recognition for structural health monitoring using time series modeling: Theory and experimental verifications." *Mechanical Systems and Signal Processing* 23, no. 7 (2009): 2192-2204.

[12] Hodge, Victoria J., Simon O'Keefe, Michael Weeks, and Anthony Moulds. "Wireless sensor networks for condition monitoring in the railway industry: A survey." *IEEE Transactions on Intelligent Transportation Systems* 16, no. 3 (2015): 1088-1106.

[13] Huang, Hai, and Erol Tutumluer. "Discrete element modeling for fouled railroad ballast." *Construction and Building Materials*25, no. 8 (2011): 3306-3312.

[14] Huang, Hai, and Erol Tutumluer. "Discrete element modeling for fouled railroad ballast." *Construction and Building Materials*25, no. 8 (2011): 3306-3312.

[15] Huang, Hai. *Discrete element modeling of railroad ballast using imaging based aggregate morphology characterization*. University of Illinois at Urbana-Champaign, 2010.

[16] Huang, Hai, Erol Tutumluer, and William Dombrow. "Laboratory characterization of fouled railroad ballast behavior." *Transportation Research Record: Journal of the Transportation Research Board* 2117 (2009): 93-101.

[17] Huang, Hai, Shushu Liu, and Tong Qiu. "Identification of Railroad Ballast Fouling through Particle Movements." *Journal of Geotechnical and Geoenvironmental Engineering* 144, no. 4 (2018).

[18] Huang, Hai, and Erol Tutumluer. "Discrete element modeling for fouled railroad ballast." *Construction and Building Materials*25, no. 8 (2011): 3306-3312.

[19] Indraratna, Buddhima, Li-jun Su, and Cholachat Rujikiatkamjorn. "A new parameter for classification and evaluation of railway ballast fouling." *Canadian Geotechnical Journal* 48, no. 2 (2011): 322-326.

[20] Indraratna, Buddhima, Nayoma C. Tennakoon, Sanjay Shrawan Nimbalkar, and Cholachat Rujikiatkamjorn. "Behaviour of clay-fouled ballast under drained triaxial testing." (2013): 410.

[21] James, Gareth, Daniela Witten, Trevor Hastie, Robert Tibshirani, and SpringerLink (Online service). *An Introduction to Statistical Learning: With Applications in R*. Vol. 103;103.;. New York, NY: Springer New York, 2013. doi:10.1007/978-1-4614-7138-7.

[22] Li, Dingqing, James Hyslip, Ted Sussmann, and Steven Chrismer. 2015. *Railway geotechnics*. Boca Raton, Fla. [u.a.]: CRC Press/Spon Press.

[23] Liu, Shushu, Hai Huang, Tong Qiu, and Yin Gao. "Study on Ballast Particle Movement at Different Locations Beneath Crosstie Using "SmartRock"." In *2016 Joint Rail Conference*, pp. V001T01A013-V001T01A013. American Society of Mechanical Engineers, 2016.

[24] Liu, Shushu, Hai Huang, Tong Qiu, and Jayhyun Kwon. "Effect of geogrid on railroad ballast particle movement." *Transportation Geotechnics* 9 (2016): 110-122.

[25] Liu, Shushu, Hai Huang, Tong Qiu, and Liang Gao. "Comparison of Laboratory Testing Using SmartRock and Discrete Element Modeling of Ballast Particle Movement." *Journal of Materials in Civil Engineering* 29, no. 3 (2017): D6016001.

[26] Selig, Ernest Theodore, and John M. Waters. *Track geotechnology and substructure management*. Thomas Telford, 1994.

[27] Sohn, Hoon, Charles R. Farrar, Francois M. Hemez, and Jerry J. Czarnecki. *A Review of Structural Health Review of Structural Health Monitoring Literature 1996-2001*. No. LA-UR-02-2095. Los Alamos National Laboratory, 2002.

[28] Sohn, Hoon, and Charles R. Farrar. "Damage diagnosis using time series analysis of vibration signals." *Smart materials and structures* 10, no. 3 (2001): 446.

[29] Sohn, Hoon, Jerry A. Czarnecki, and Charles R. Farrar. "Structural health monitoring using statistical process control." *Journal of structural engineering* 126, no. 11 (2000): 1356-1363.

[30] Somwanshi, S., and B. Gawalwad. "Monitoring civil structures with a smart wireless sensor network." *International Journal of Engineering and Applied Sciences* 3 (2016): 34-39.

[31] Suiker, Akke SJ, Ernest T. Selig, and Raymond Frenkel. "Static and cyclic triaxial testing of ballast and subballast." *Journal of geotechnical and geoenvironmental engineering*131, no. 6 (2005): 771-782.

[32] Tennakoon, Nayoma, Buddhima Indraratna, Cholachat Rujikiatkamjorn, Sanjay Nimbalkar, and Tim Neville. "The role of ballast-fouling characteristics on the drainage capacity of rail substructure." *Geotechnical Testing Journal* 35, no. 4 (2012): 629-640.

[33] Zarembski, Allan M., Gregory T. Grissom, and Todd L. Euston. "On the Use of Ballast Inspection Technology for the Management of Track Substructure." *Transportation Infrastructure Geotechnology* 1, no. 1 (2014): 83-109.

[34] Qian Y, Mishra D, Tutumluer E, Hashash YA, Ghaboussi J. Moisture Effects on Degraded Ballast Shear Strength Behavior. ASME. ASME/IEEE Joint Rail Conference, 2016 Joint Rail Conference ():V001T01A034. doi:10.1115/JRC2016-5840.

[35] Welling, Max. "Fisher linear discriminant analysis." Department of Computer Science, University of Toronto 3, no. 1 (2005).

[36] https://onlinecourses.science.psu.edu/stat510/node/62

[37] from http://sebastianraschka.com/Articles/2014_python_lda.html